5. THERMAL ANALYSIS INSTRUMENTATION AND APPLICATIONS

5.1. Introduction

Present day thermal analysis instrumentation has reached a high state of sophistication compared to the instruments that were available 15–20 years ago. The investigator has a wide range of commercial instruments to choose from, covering the temperature range from −150 to 2400°C. Numerous instruments have also been described in the literature which can extend this temperature range in either direction.

The instruments discussed in this chapter include only those that have been described in the literature during the past 5–6 years. No attempt is made to discuss the fundamental principles of each technique as these are adequately reviewed in the many textbooks that are available. The discussion is not comprehensive but tends to emphasize only those instruments that are commonly used to study heterogeneous processes.

5.2. Thermogravimetry

The most widely used thermal technique to study heterogeneous processes is that of thermogravimetry (TG). It is a limited technique, however, in that a gas–solid system must be involved in which the gaseous component is either a reactant or product of the reaction. Phase transitions such as solid → gas may also be investigated by this technique. Data obtained from TG are more quantitative, say, than differential thermal analysis (DTA). In the latter technique, the differential temperature response decreases with increasing temperature of the system. In a well designed and constructed thermobalance, this is not present: the mass-response is invariant with temperature.

No attempt will be made here to discuss all of the aspects of TG instruments. The historical development and principles of the thermobalance have been well documented by numerous authors[1–8] while modern commercial instruments have been described in detail by Wendlandt[9] and others[10,11]. Only the more recent or novel approaches or developments of TG instrumentation will be discussed here as well as their applications.

5.2.1. Temperature measurements and calibration

The use of TG for kinetics studies has created problems involving sample temperature measurements. For heating rates of 150 to 600°C/h, sample temperatures may lag behind furnace temperature from 3 to 14°C[12]; in vacuum systems it is not unusual to have differences of up to 20°C. The accuracy requirements in reaction kinetics are stringent and require that the temperature of the sample be determined directly while it is being weighed continuously. Some thermobalances have provision for this in that a thermocouple is in intimate contact with the sample or sample container. In other instruments, the temperature of the furnace chamber only is continuously monitored.

Manche and Carroll[13] developed a fast response transducer in physical contact with the sample in which its temperature information is instantaneously relayed to an indicating device through a non-mechanical coupling. It consists of using a uni-junction transistor relaxation oscillator with a thermistor as the resistive part. The entire primary circuit including the power supply is made part of the balance suspension and is weighed along with the sample. The frequency of oscillation, which is a function of sample temperature, is relayed to an events-per-unit-time meter via a mutual inductance between two suspended coils. Unfortunately, the temperature range covered was rather limited, from 25 to 160 °C.

Norem et al.[14,15] described the use of substances having magnetic transitions for the temperature calibration and performance evaluation of a TG system. The ferromagnetic standards is suspended from the balance beam in a magnetic field which is oriented so that a vertical component of magnetic force acts on the sample. When the sample is heated through its Curie point, the equivalent magnetic mass diminishes to effectively zero and the balance will indicate an apparent weight-loss. The magnetic transition calibration points are shown in Table 5.1 while a typical calibration curve is illustrated in Fig. 5.1. The intersection of a line drawn through the rapidly changing

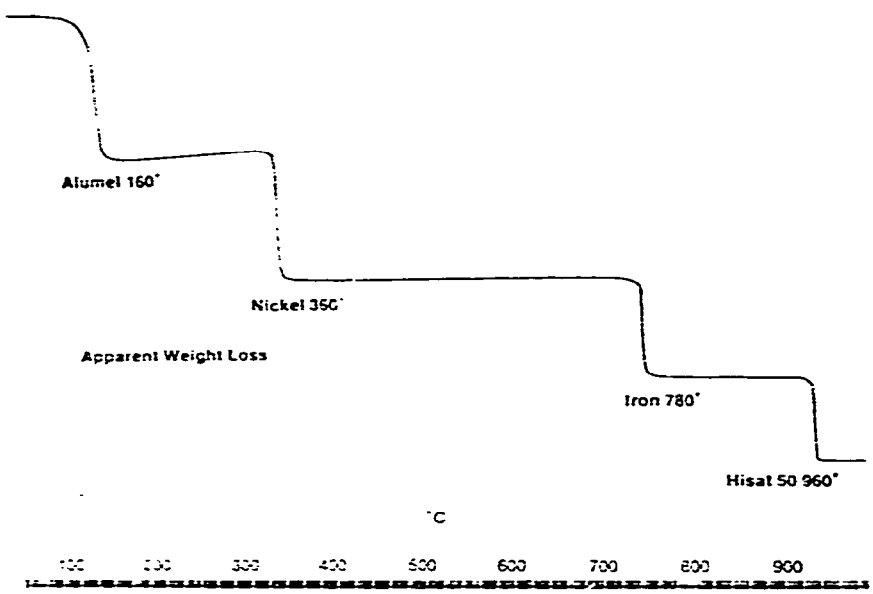

Fig. 5.1. Temperature calibration with magnetic standards (10 °C/min)[15].

portion of the curve and a line extrapolated backwards from the horizontal baseline above the transition was taken as characterizing the transition point. It was found that this point was reproducible to within ±1 °C and was independent of sample size and magnetic field strength within the ranges of interest.

5.2.2. Environmental factors

As is well known, the experimental transition temperatures, and in some cases

TABLE 5.1
MAGNETIC TRANSITION CALIBRATION POINTS[15]

Standard	*Transition temperature (°C)*
Alumel	163
Nickel	354
Perkalloy	596
Iron	780
HiSat 50	1000

the shape, of a TG curve are profoundly altered by a change in furnace atmosphere. The composition and pressure of the gaseous atmosphere within the sample-furnace chamber can be varied over a wide range. Most easily employed are non-corrosive gases such as air, argon, nitrogen, oxygen, hydrogen, carbon dioxide, and so on, but provision is made in certain instruments for studies in corrosive atmospheres such as HCl, Cl_2, SO_3, etc. Not only can a wide variety of gaseous atmospheres be employed, but the pressure in the system can be varied from $\sim 1 \times 10^{-6}$ torr to about 200 atm.

Self-generated TG atmospheres have been reviewed by Newkirk[16]. This type of atmosphere consists of decomposing a solid sample in a crucible that has a small vapor volume with a small opening to the atmosphere. As a consequence, except for the air initially present, decomposition occurs in an atmosphere of the gaseous decomposition products, hence, a self-generated atmosphere. The review outlines the advantages and limitations of the method, describes several new crucibles, and compares the results obtained for various chemical systems. The self-generated atmosphere method has a sound theoretical basis, and in such cases, would seem to be a good choice for the initial TG study of a complex solid–gas system. In a self-generated atmosphere crucible the atmosphere produced by the first reaction may have a beneficial or detrimental effect on the reaction. For example, in consecutive

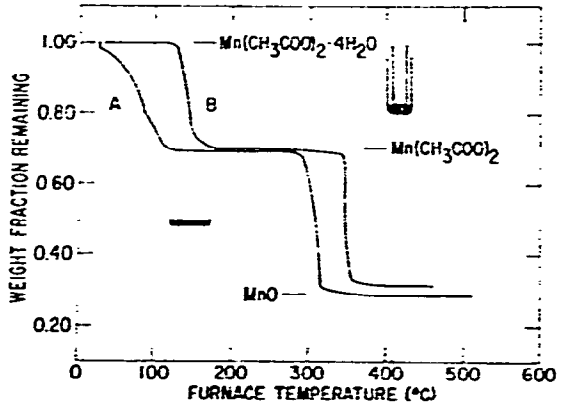

Fig. 5.2. TG curves of $Mn(C_2H_3O_2)_2 \cdot 4H_2O$. A: Shallow dish of sample in flowing N_2; B: Piston type sample crucible in air[16].

hydrate decompositions the presence of water vapor facilitates the recrystallization of the new phase.

To illustrate[16] the effect of the self-generated atmosphere on the decomposition of a compound, the curves for manganese(II) acetate 4-hydrate are shown in Fig. 5.2. In curve A, the sample loses weight immediately at room temperature. The two major stages of weight-loss on heating correspond approximately to the loss of hydrate water and the decomposition of the anhydrous salt to MnO. The effect of the self-generated atmosphere, as shown in Curve B, is to increase the initial weight-loss temperature and also the temperature at which the anhydrous salt dissociates.

The advantages and limitations of the self-generated atmosphere technique, as listed by Newkirk[16], are as follows:

A. Advantages

a. TG in self-generated atmospheres is primarily of value in the study of consecutive reactions. It will generally have the following advantages compared to TG in open crucibles.

1. The reaction interval will be narrower, overlapping reactions will be more clearly resolved, and intermediates more accurately identified.

2. New phases will be revealed.

3. Reactions will proceed, for the most part, at a fixed pressure of the gaseous products equal to atmospheric pressure. The course of reactions, except at the start, will not be affected by varying partial pressure.

4. The observed initial decomposition temperature will be more closely related to an equilibrium decomposition temperature.

5. The results will be more directly comparable with results from separate differential thermal analysis experiments.

6. Experiments can be performed on materials subject to oxidation at elevated temperatures with little interference from oxidation.

7. Very fast reactions can be studied without loss of solid product.

8. Better results will be obtained on materials with an appreciable vapor pressure at room temperature. The sample can be weighed more accurately and will yield a horizontal baseline on the thermogram.

9. The effects of particle size differences will be reduced and the effects of crucible geometry standardized. This is particularly important with inhomogeneous materials such as rocks and minerals.

10. The recrystallizations of new phases from hydrates or hydroxides will be facilitated.

11. It has been claimed that irreversible decompositions will show better resolution and a smaller reaction interval in some instances, though it is not known why.

b. Thermogravimetry in self-generated atmospheres also has some advantages over controlled atmosphere thermogravimetry.

1. The balance need not be protected from condensible or corrosive gases.

2. No additional apparatus is needed except the sample holder.

3. The advantages of controlled atmosphere thermogravimetry are available even when different stages require different atmospheres.

4. The advantages of controlled atmosphere thermogravimetry are available even when the gaseous product is a mixture or is unknown.

B. Limitations of thermogravimetry in self-generated atmospheres

1. Buoyancy corrections vary depending on the molecular weight of the gas filling the crucible.

2. Large, heavy crucibles will cause a greater uncertainty in sample temperature.

3. In dehydration of hydrates, the chances of melting and the appearance of pseudo-plateaus may be enhanced.

4. Poorer resolution may result if the first reaction is delayed to a temperature at which a subsequent reaction begins.

5. Secondary reactions with the evolved gas may make interpretation difficult.

C. Recommended uses

Thermogravimetry in self-generated atmospheres may be useful for studies of:

1. Consecutive reactions, and particularly for hydroxides, hydrates, ammoniates, carbonates, acetates, oxalates, and sulfates.

2. Inhomogeneous materials.

3. Compounds that decrepitate or explode.

4. Air sensitive materials.

5. Volatile materials.

6. Materials that decompose to yield several gaseous products.

7. Destructive distillation.

The effect of various gaseous atmospheres on thermal decomposition reactions using the Mettler thermobalance has been discussed by Wiedemann and co-workers[17–19]. The gas flow and control system for the Mettler thermobalance is illustrated in Fig. 5.3. For atmospheric or vacuum applications, non-corrosive gases are passed through the balance housing, and then up into the sample chamber. Upward passage of the gas prevents diffusion of the reaction gases back into the balance case or condensation of solids or liquids on the support rod. The effect of gas flow on the weight measurements is quite small, being approximately 0.3 mg at the

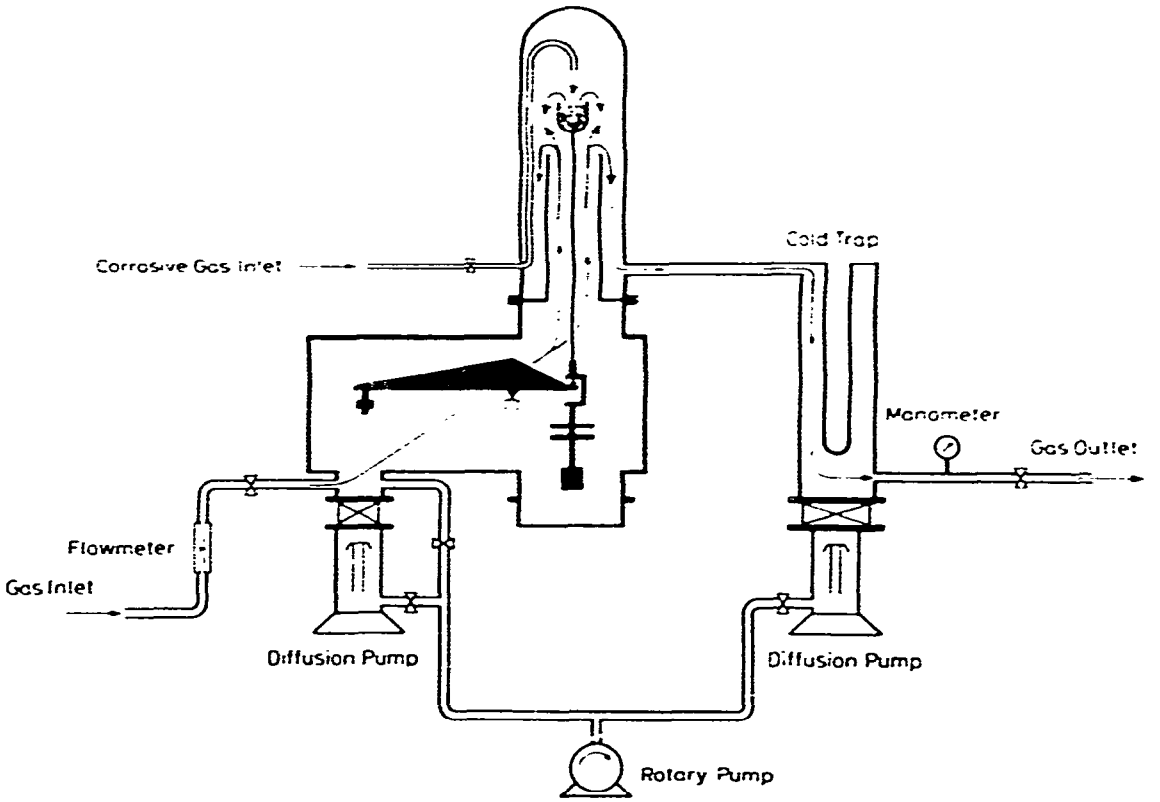

Fig. 5.3. Mettler thermobalance gas flow and control diagram.

maximum flow rate of 700 ml/min and 0.1 mg at 160 ml/min. TG curves can also be obtained in vapor atmosphere[20,21] (such as H_2O or D_2O) or in corrosive gas atmosphere[19] (chlorine, for example).

Gulbransen et al.[22] have described a flow-reaction system and gas-handling system employing a Cahn RG balance. Pressures of 2 to 76 torr and flow rates of 5×10^{18} to 1.8×10^{20} molecules of oxygen per second were employed in the system.

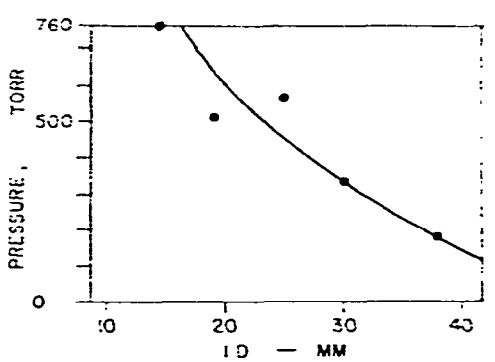

Fig. 5.4. Effect of pressure for 1 μg peak-to-peak noise[22]

Conditions for optimum sensitivity in TG at atmospheric and reduced pressures have been investigated by Cahn and Peterson[23]. The effect of pressure as a function of furnace tube diameter is shown in Fig. 5.4. If larger furnace tubes must be employed, a gas pressure as high as possible should be used. Baffles were tried but found to be of little value in reducing the noise. Noise as a function of tube diameter seemed to be the same with flowing gases as with static ones. It appears that the noise is nearly independent of gas velocity through the system. In another investigation[24], the effect of pressure on aerodynamic noise was determined. At pressures up to 150 torr the noise was not more than 1 μg peak-to-peak; above 200 torr, the noise increased rapidly. In a related study, the errors encountered in vacuum TG were discussed by Friedman[25]. The effect of momentum transfer was described, which can be related to the equation:

$$w = m - \left(\frac{1}{g}\right) \alpha \left(\frac{dm}{dt}\right) \tag{5.1}$$

Where w is the weight as read by the balance, m is the actual weight of the sample, g the acceleration due to gravity, α the geometric factor, and dm/dt the rate of change of actual weight. This effect was measured by supporting polymer film samples both above and below the sample container of the thermobalance. The results indicate that errors caused by lift effects were due to molecules which migrate to regions below the container as they are pumped past it and the support wire. Improved design could probably reduce the tendency of molecules to migrate below the container.

5.2.3. Sample containers

The various factors of heat transfer (heat exchange between the reaction interface and the source of heat), the temperature gradients in the sample, and mass transfer are all related to the sample holder geometry. Many different geometrical configurations have been prepared, however, only several illustrative examples will be given here.

Šesták[26,27] calculated the maximum temperature gradients between the wall of the sample holder and the center of the sample, Y_m. For a disc sample

$$Y_m = \left[\frac{\Delta HG\theta}{\lambda}\left(\frac{S}{2}\right)\right]^{1/2} \tag{5.2}$$

and for a cylindrical sample

$$Y_m = \frac{\Delta HG\theta}{2\lambda} r \tag{5.3}$$

where ΔH is the enthalpy change, G the sample heat capacity, θ the heating rate, λ is the reciprocal of the sample heat conductivity, S the thickness, and r the diameter. For a cylindrical sample of 1 mm diameter, placed in a silver block, at a heating rate of 5 K/min, the maximum temperature gradient found was: (a) 4.8 K for the de-

hydration of kaolin; (b) 13.2 K for the decomposition of magnesite; and (c) 3.1 K for the dehydration of α-$CaSO_4 \cdot 0.5H_2O$. The amount of sample influences the enthalpy change during the reaction in the sample and is able to slow down (or speed up) the temperature increase from that of the furnace heating rate. In the former case, the errors of self-cooling of the sample must be taken into account. The self-cooling is a function of sample load, enthalpy change of the reaction, and the thermal inertia of the sample container. Šesták[26] calculated for a 0.15 g of kaolin in a silver crucible at a heating rate of 5 K/min, that the temperature increase was slowed down by about 1 K/min. It is possible to estimate the optimum amount of sample by means of a semi-empirical method[27], under any given experimental conditions.

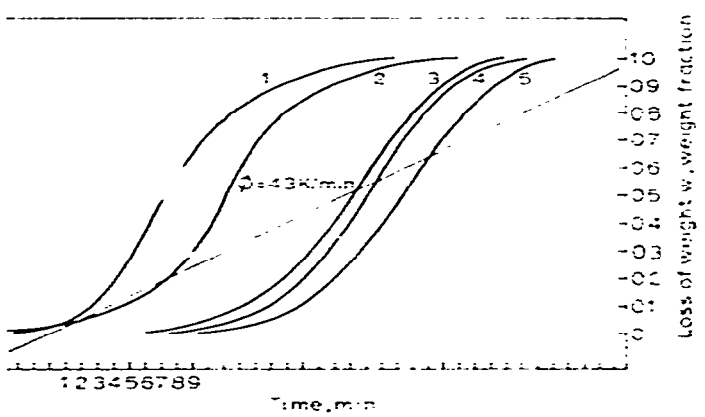

Fig. 5.5. Decomposition of kaolin under various experimental conditions[26]. (1) Multi-plate silver holder in dynamic air atmosphere; (2) Same as (1) except static air atmosphere; (3) Perforated silver block, 3 mm capillaries; (4) Same as (3) but 6 mm capillaries; (5) Same as (3) but 10 mm capillaries.

The importance of mass transfer is shown in Fig. 5.5 in which TG curves of kaolin are given under various experimental conditions[26]. The sample is spread in a thin layer on the plates of a multi-plate silver sample holder in curves (1) and (2). The influence of diffusion in the sample is shown by curves (3)–(5) in which the surface area exposed to the atmosphere is reduced by the use of capillary tubes of varying length (3 to 10 mm). From these studies, Šesták[26] recommends the use of a thin layer of sample spread out on the plates of a multi-plate sample holder.

The various sample holders used in Derivatography, as shown in Fig. 5.6, were discussed in a lengthy review by Paulik et al.[28]. To resolve or separate overlapping reactions, Paulik et al.[28–30] recommended the use of the multiplate sample holder. They reasoned that if the sample is spread out in a thin layer to permit rapid transport of the gaseous decomposition products away from the vicinity of the solid phase, then the decomposition processes occurred not only at lower temperatures but also over a smaller temperature interval. Thus, there would be a better resolution of overlapping processes. Such an increase in resolution can be seen in the curves in Fig. 5.7. The multiplate curve shows that the dehydration takes place in three stages while the crucible curve only exhibits two stages of dehydration. Using other chemical systems,

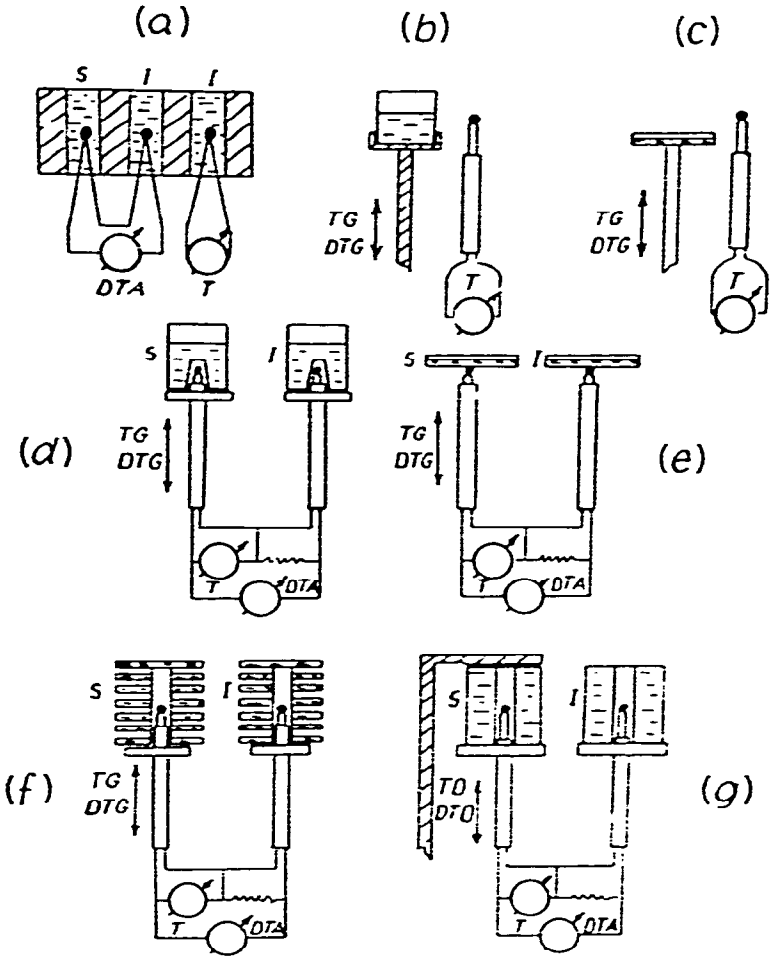

Fig. 5.6. Sample holders used in Derivatography[28]. a, block type; b, crucible; c, plate; d, crucible; e, plate; f, multiplate; g, compressed sample.

it was found that phase transitions such as solid → liquid were nearly independent of changes in experimental conditions using the multiplate sample holder. Other multiplate sample holders for TG have been described[34,35].

Wiedemann[31] described the various sample holders used in the Mettler thermobalance: these are illustrated in Fig. 5.8. Crucible materials were selected to obviate the possibility of reaction between crucible and sample material. Materials used were platinum, alumina, quartz, and graphite. All crucibles made contact with the temperature measuring thermocouple at the base and were readily interchangeable with each other.

Looking at other variables, as well as the sample container geometry, Wiedemann et al.[32] argued that in order to obtain valid and consistent results in the determination of activation energies, a number of precautions must be taken in the preparation and handling of the sample. He listed them as:

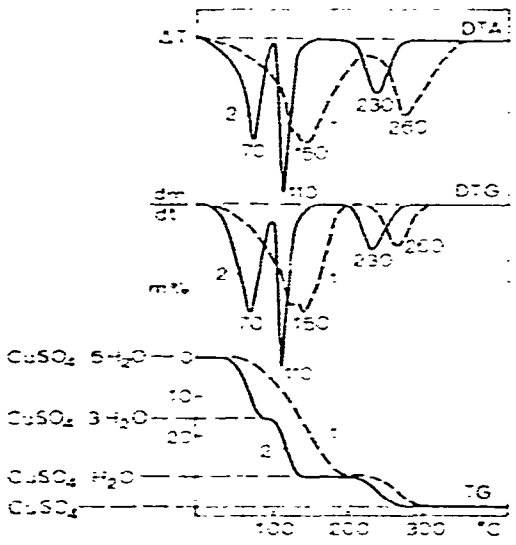

Fig. 5.7. Comparison[25] of crucible and multiplate sample holders for $CuSO_4 \cdot 5H_2O$. Curve 1, crucible (500 mg); curve 2, multiplate (200 mg).

A. Use of a sample small enough to ensure temperature uniformity during the decomposition and, of course, direct sample temperature measurement.

B. Adjustment of the gas flow and pressure and sample shape to reduce the effects of effluent gases from the sample.

C. Uniform sample particle size and sample packing in the crucible.

The influence of sample packing in the sample holder on the dehydration of $CaC_2O_4 \cdot H_2O$ was cleverly demonstrated by Wiedemann[33]. Using three different types of sample packing, the dehydration, as indicated by the water evolution curves, takes place over different temperature ranges, as shown in Fig. 5.9. Sample packing (A) and (B) lead to almost symmetrical peaks with rapid dehydration. For packing (C), complete dehydration is delayed, leading to a peak temperature shift of about 80°C.

A word of caution was expressed by Ramakrishna Udupa and Aravamudan[36] concerning the use of platinum sample holders. Platinum, because of its catalytic activity, may modify to an appreciable extent the TG curve of a compound and that this should be taken into account in the interpretation of the data.

5.2.4. Simultaneous TG techniques

Simultaneous thermal analysis measurements on the same sample under identical pyrolytic conditions have numerous advantages[37]. The most common simultaneous technique is that involving TG–DTA, although TG–gas evolution analysis is also becoming quite popular. The latter usually involves a mass spectrometer to analyze the volatile products but gas chromatography has also been employed.

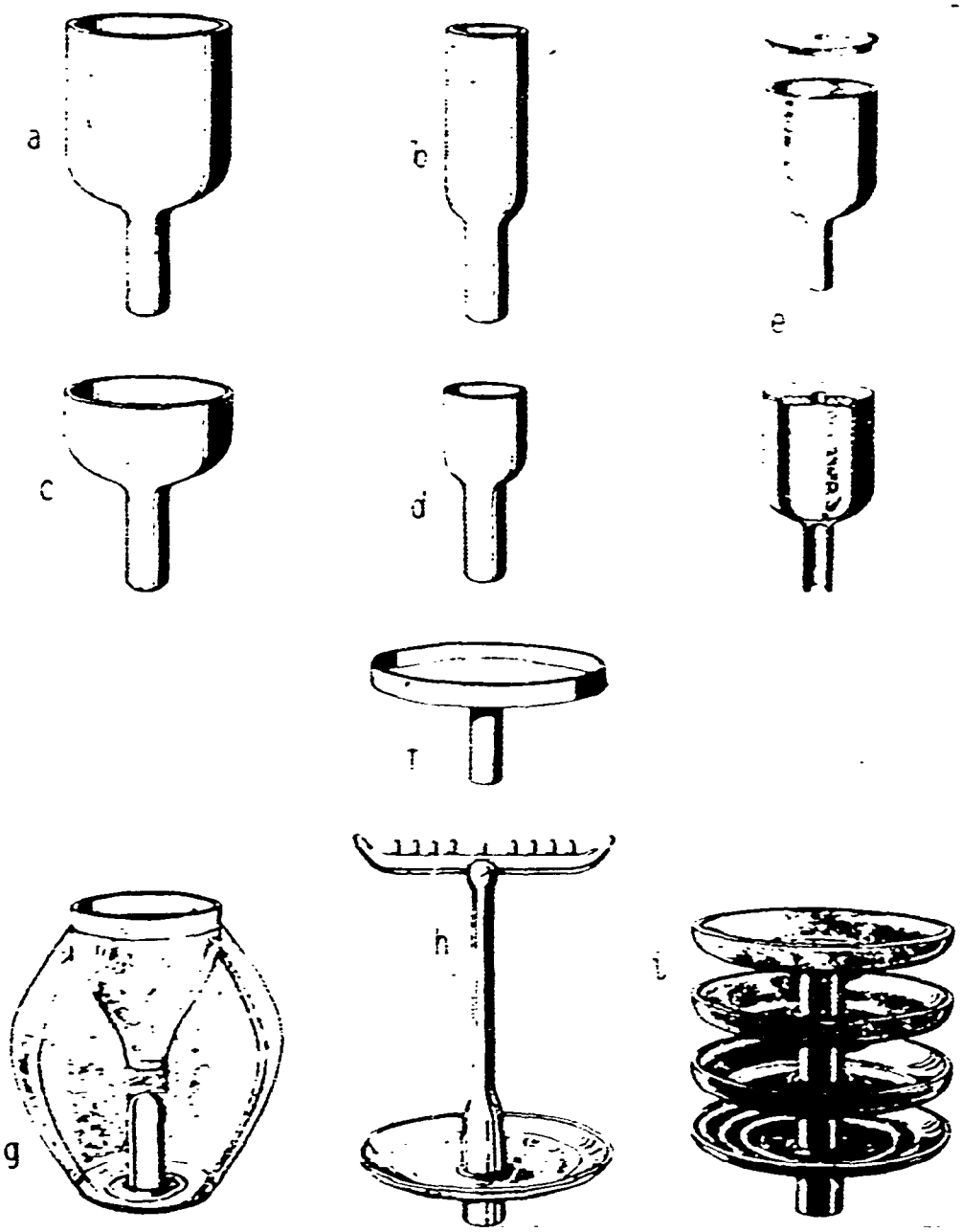

Fig. 5.8. Sample holders used in the Mettler thermobalance[31].

Simultaneous TG–DTA instruments have been described[34,35,41,50] while the significance of their measurements has been discussed[38]. According to Maurer and Wiedemann[38], simultaneous studies using carefully planned combinations according to the system under investigation will help and improve the interpretation of the results.

The combination of a thermobalance with a gas chromatograph has been

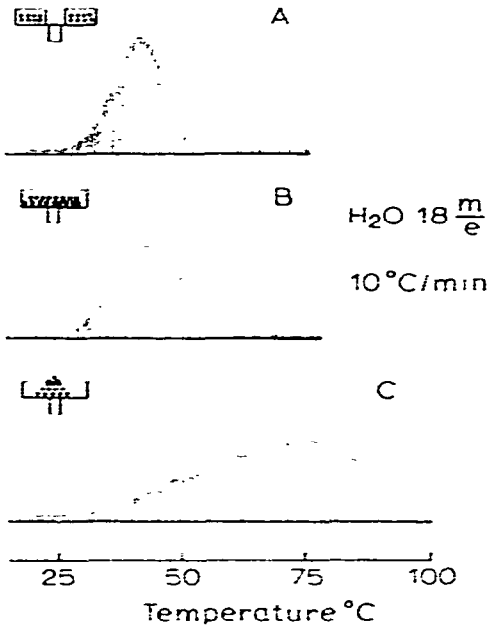

Fig. 5.9. Release of water from $CaC_2O_4 \cdot H_2O$ as a function of sample packing[33].

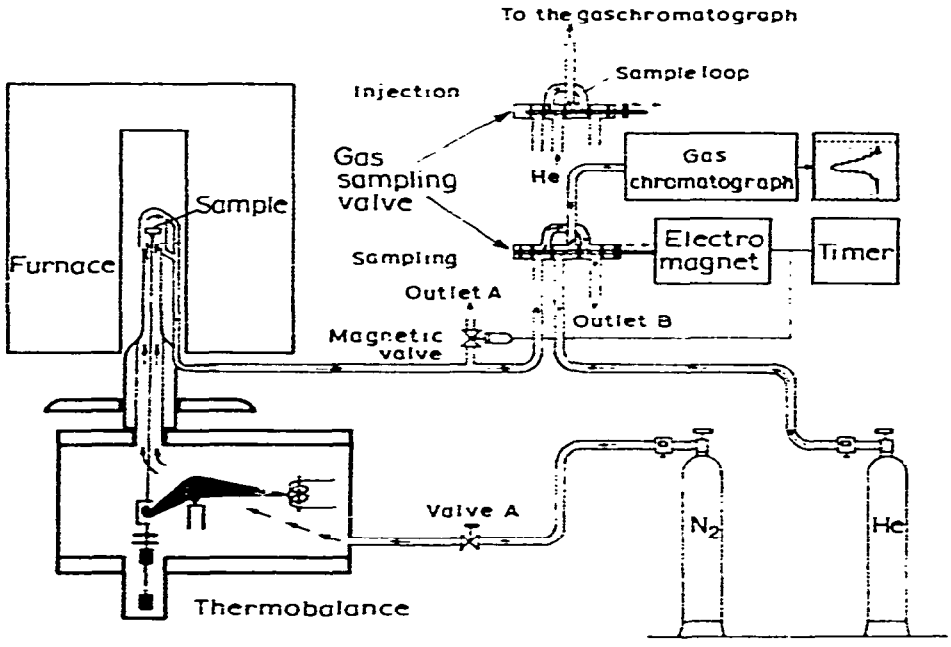

Fig. 5.10. Simultaneous TG–GC technique used by Wiedemann[33].

described by several investigators[33,39,40]. The apparatus used by Wiedemann[33], as shown in Fig. 5.10, consists of a Mettler thermobalance connected to a gas chromatograph. Evolved gaseous reaction products are sampled by the sampling valve which can be opened at specific intervals. Helium gas then flushes the reaction gases into the

gas chromatograph for analysis. Wiedemann[33] concluded that compared to mass spectrometric analysis, the gas chromatograph method of analysis is much slower but that the quality of the results is about the same.

The use of a mass spectrometer to analyze the evolved gases has been described by a number of workers[33,35,43-46,51]. The system used by several of the investigators[33,43] is shown in Fig. 5.11. The Mettler thermobalance is coupled to a Balzers Quadrupole mass spectrometer. Gaseous decomposition products come into

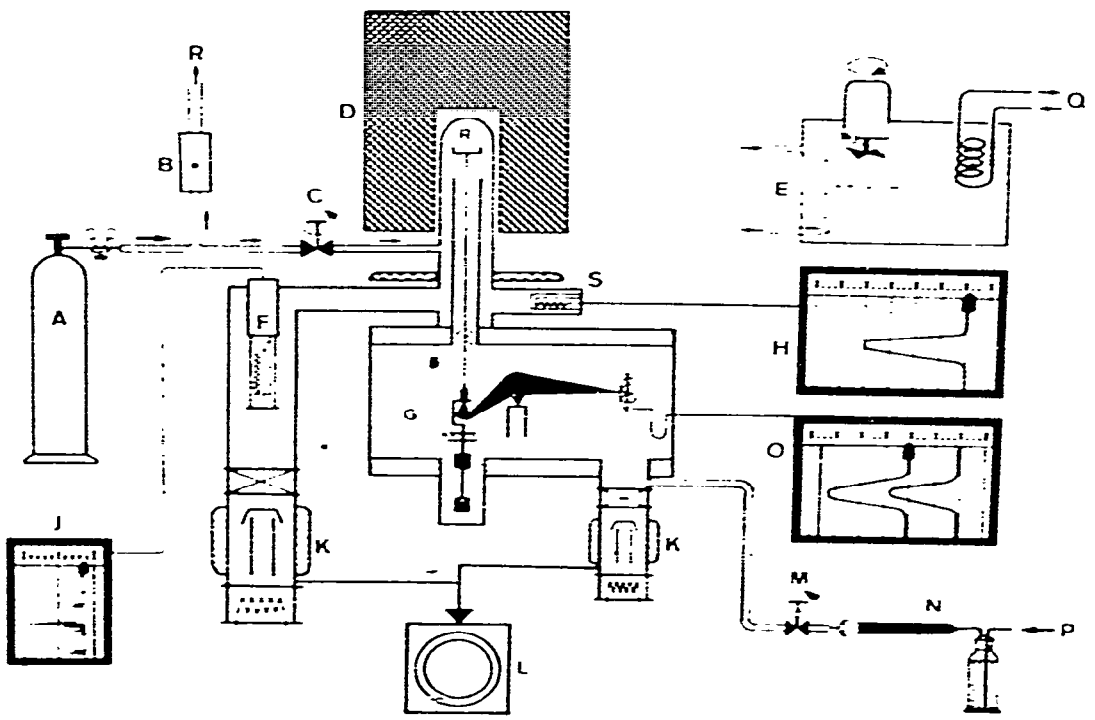

Fig. 5.11. TG–mass spectrometer system used by Wiedemann[33] and Gibson and Johnson[43].

immediate contact with the mass analyzer. Pressure range in the system is 10^{-4} to 10^{-6} torr while the mass range covered is 1–100 or 10–400 amu. It is possible not only to scan the entire spectrum range but also to monitor a single m e value. The TG–MS measurements of $CaC_2O_4 \cdot H_2O$ are illustrated in Fig. 5.12. Contrary to the decomposition reaction carried out in a dynamic air atmosphere, the decomposition temperatures for the two reversible processes, dehydration and decomposition of $CaCO_3$, are shifted 175 to 80 °C, and 760 to 650 °C, respectively. The irreversible oxalate decomposition takes place at the same temperature of 470 °C. It is also seen that during the CaC_2O_4 decomposition, disproportionation takes place according to the equation:

$$2CO \rightleftarrows C + CO_2 \qquad (5.4)$$

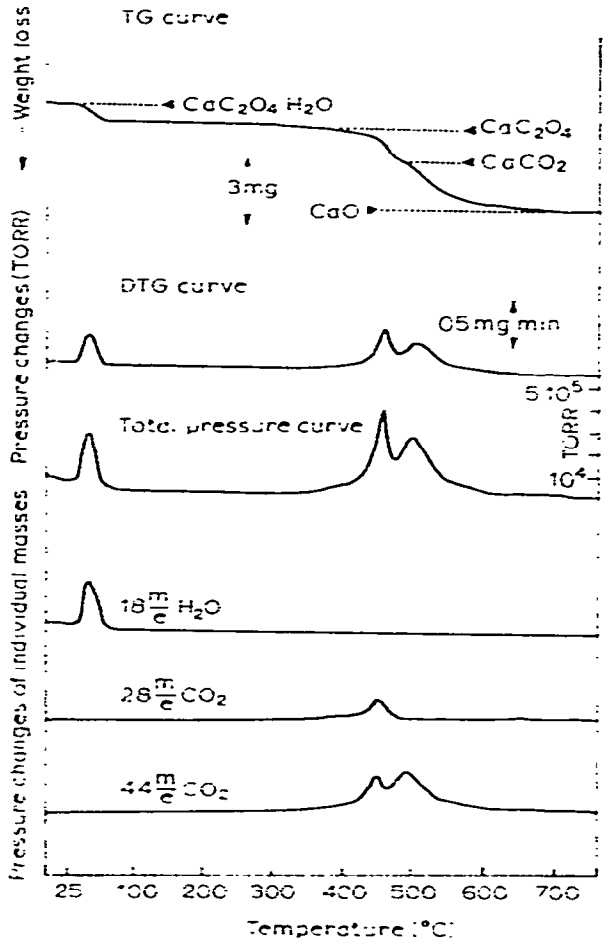

Fig. 5.12. TG–MS curves of $CaC_2O_4 \cdot H_2O$ according to Wiedemann[33].

Loss of CO_2 from the $CaCO_3$ takes place very slowly and is retained, due to physical adsorption, at 600 and until about 700 C.

Gibson[44] described the application of a small on-line computer to control the mass spectrometer.

Using the Derivatograph, Paulik and Paulik[47–49] described an apparatus for the recording of the temperature (T), DTA, TG, differential thermogravimetry (DTG), thermo-dilation (TD), differential thermo-dilation (DTD), thermo-gas-titrimetric (TGT), and differential thermo-gas-titrimetric (DTGT) curves.

A simultaneous TG and X-ray apparatus was described by Wiedemann[52].

Thermobalances for the measurement of vapor pressure[53] and dissociation pressures[54], high temperature materials research[55,56], high pressure studies[57], and low pressure studies[58] have been described.

Bradley and Wendlandt[60] predicted, perhaps, the future of thermogravimetry instrumentation by describing a completely automatic thermobalance. Eight consecutive samples could be studied without the attention of the operator. Automatic

sample changing can be carried out as well as compositional changes of the flowing gaseous atmospheres.

5.3. Differential thermal analysis

The instrumentation for differential thermal analysis (DTA) has been discussed in detail in well known reference books[3,62–66] and has been reviewed in detail by Murphy in biennial reviews, the latest of which appeared in 1972[67]. Commercial instruments have been described by Gordon[68] and Wendlandt[9,69] as well as others[11]. No attempt will be made here to discuss the basic principles of the instrumentation but rather to review the more recent developments.

5.3.1. Sample holder geometry and thermocouples

Perhaps the most important aspect of DTA instrumentation is that of sample holder geometry, thermocouple configuration and placement, and their materials of construction. Great interest, as evidenced by the number of publications which have appeared in recent years, has been shown in this aspect of instrumentation. Thus, it is important to consider them first.

The sample holders developed for the Stone DTA systems (now Columbia Scientific Industries) are shown in Fig. 5.13. As is well known, one of the configurations (A) permits the flow of gases directly through the sample during the heating

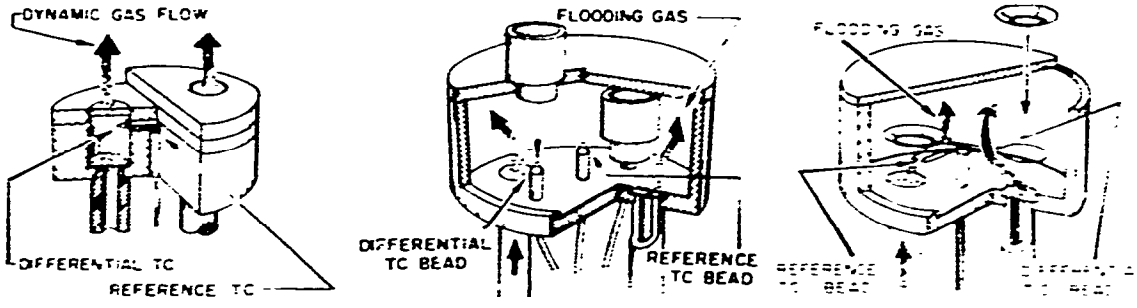

Fig. 5.13. Sample holder arrangements for the Stone system instruments. (A) Dynamic gas flow types; (B) cup type; (C) ring-thermocouple type.

cycle. This configuration is used for powdered minerals and other samples which do not undergo sintering or fusion. For samples which undergo solid → liquid transitions or for liquids, the cup type holder (B) is employed. Highest sensitivity is achieved by the use of the ring-type thermocouple (C). The sample is placed in a shallow crucible or dish which is in direct contact with the thermocouple junction.

Wiedemann and van Tets[70–72] have discussed the sample holders used for the Mettler TG–DTA instrument. According to these investigators, the choice of sample holder for DTA is often a compromise, depending upon the type of reaction under investigation. The flat plate type, which is ideal for control of the gas–solid reaction in TG, may cause loss of ΔT sensitivity through radiant heat loss. For a solid$_1$ → solid$_2$

transition, where the furnace gaseous environment plays no role, a spherical holder might be ideal for measuring a maximum ΔT but it is difficult to construct or to load. The closest practical approach to the latter shape is a cylinder of a 1:1 height:diameter ratio. If the cylindrical crucible is welded to the thermocouple, a maximum ΔT signal will be transferred to the measuring system. Use of small samples ($\simeq 0.03\ cm^3$) in a 1:1 cylinder still permits adequate gas exchange with maximum heat retention for differential temperature measurements. Sample holders used in the Mettler system are shown in Fig. 5.14.

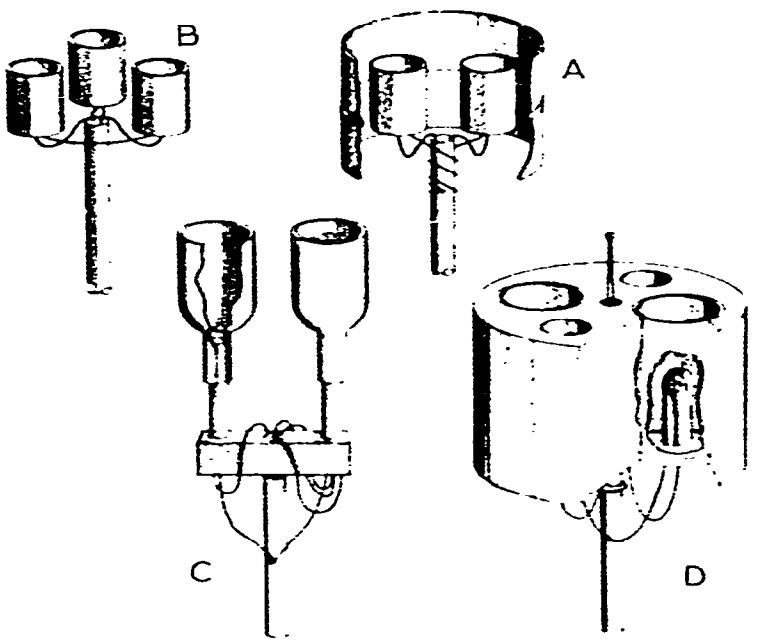

Fig. 5.14. Sample holders used by Wiedemann[70,71]. (A) Micro TG–DTA for vacuum; (B) Micro TG–DTA holder; (C) Macro TG–DTA holder; (D) Macro TG–DTA type with heat sink block.

Ozawa and co-workers[73–75] designed a number of sample holders which had first been described mathematically. One such holder contained a twenty junction thermopile[75]. Sealed tube sample holders for DTA have been described recently by Barrett et al.[76,77] and Wendlandt[78]. The sealed tubes prevent vaporization and sublimation reactions from occurring which frequently interfere with or alter other types of chemical reactions.

In order to permit the passage of gas through a sample, such as is employed in the Stone equipment, Karkhanavala et al.[79] proposed the use of a sample holder constructed of platinum wire gauze. This type of sample holder gave curves whose peaks were extremely sharp and of greater intensity than when solid metal crucibles were used. These sample holders could be used for TG studies also.

The design of sample holders has been considered by several investigators[80–82]. Mathematical models were developed which were then applied to practical instrument

configurations. Dosch[83] described a simple electrical device to measure heat sensitivity and response time of a DTA sample holder. For an isolated crucible type sample holder, a simple electrical calibration technique was used which introduced a measured amount of electrical power into the crucible and then measured as a response the change in its temperature.

Thin film thermocouples for DTA measurements were discussed by King et al.[84,85]. Light weight, precisely matched thermocouples were prepared by the evaporation of thin films of dissimilar metals which overlapped to form the thermojunctions. The two metals used, gold and nickel, formed a thermoelectric junction whose e.m.f. output was intermediate between Pt–Pt (ten percent Rh) and Chromel–Alumel junctions.

In the block type sample holders, one of the greatest variables for quantitative DTA accuracy is the sample packing density factor (PDF)[86]. The effects of this PDF may be divided into two categories: (*a*) those concerned with gaseous phase interchange and (*b*) those concerned with concomitant changes in thermal diffusivity due to increased heat transfer with increased particle to particle contact. The latter effect is more generalized in that it is operative throughout the temperature range, affects base line drift and the magnitude of the reactions, but does not directly affect the temperature at which the reactions take place. A precision sample loading device was developed which readily allowed reduction in variations in technique and previously unaccounted heat losses. The device formed cylindrical samples of uniform size with closely controlled packing densities in which the thermocouple occupied a central position. An envelope of loosely packed porous granular Al_2O_3 supported the sample in the center of a metal thermal well.

The effect of thermocouple location on temperature measurement and also peak area has been investigated[72,87,88]. David et al.[87], using the Stone DSC cell, attached a digital temperature indicator to the recording system to obtain a resolution of ± 1

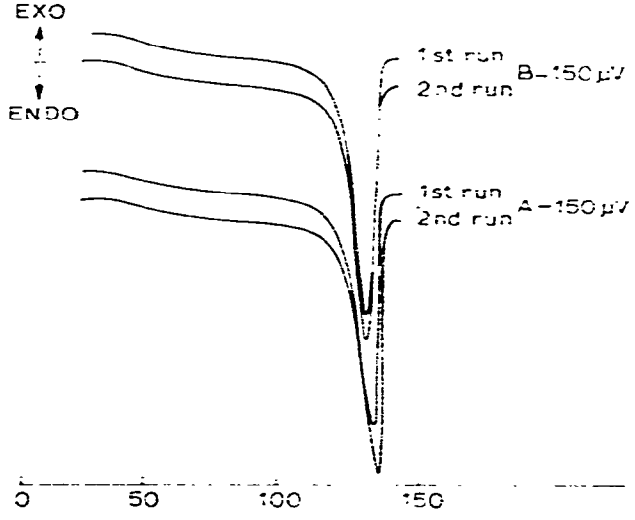

Fig. 5.15. Effect of thermocouple placement for polyethylene[87]. A = mode 1; B = mode 2.

over the temperature span from 25 to 1600 C. The effect of thermocouple placement in a sample of polyethylene is shown in Fig. 5.15. In mode 1 (curve A), ΔT is plotted against furnace temperature while in mode 2 (curve B), ΔT is plotted against sample temperature. The peak temperature always occurred at a lower temperature when mode 2 was used (for a X–Y recorder). When mode 1 is used, there is always the question of uniformity of sample holder temperature which can affect the accuracy of transition temperature measurements.

Berg and Egunov[88] found that the calculated heat of transformation is independent, within the limits of experimental error, of the mass, bulk density, specific heat and conductivity of the sample as well as of the position of the junction of the thermocouple. No corrections, in the equation which they proposed, were needed in connection with variations of these parameters.

5.3.2. High pressure DTA instrumentation

Differential thermal analysis measurements at high pressures (to 44 000 bar) have been described by several investigators. Most of the studies have been concerned with qualitative and quantitative determinations of phase equilibria and heats of transformation or heats of reaction in the temperature range of −30 to 1200 C.

Harker[89] described a high pressure DTA apparatus in which the sample was enclosed in malleable noble-metal capsules which were placed in a pressurized micro-reactor. The sample under investigation and an inert standard (MgO) were sealed in platinum capsules in the base of which was welded a platinum-13 percent rhodium wire. These wires were led from the micro-reactor through a high pressure packing gland. To complete the differential thermocouple circuit, the capsules were joined by a platinum wire. Nitrogen was used to pressurize the chamber to 1000 bar, while the maximum temperature of the system was about 900 C.

Cohen et al.[90] described a DTA system using a piston-cylinder apparatus for operations up to 44 000 bar. A three wire thermocouple assembly was employed, one junction of which was in contact with the sample. Pressure was transmitted to the sample by the furnace assembly, a combination of parts made of talc, graphite, pyrophyllite, thermocouple tubing, thermocouples, sample container, boron nitride, etc. The problems of material design, operation, and interpretation of high pressure DTA were discussed in detail.

A rather elaborate high pressure DTA apparatus was described by Kuballa and Schneider[91]. The DTA furnace and sample holders are shown in Fig. 5.16. The pressure cell was made of stainless steel and was constructed for use to maximum pressures of 4000 bar in the temperature range of −30 to 500 C. As shown in the figure, the cell was enclosed by two Bridgman type pistons in which two sheathed thermocouples were soldered to the lower piston. Two identical DTA sample holders, constructed of platinum/iridium or teflon, were attached to the thermocouple junctions. Upper and lower sides of the measuring zone were thermally insulated by low heat-conducting ZrO_2 blocks. A heating block around the pressure vessel permitted linear heating rates from 0.2 to 10 C/min.

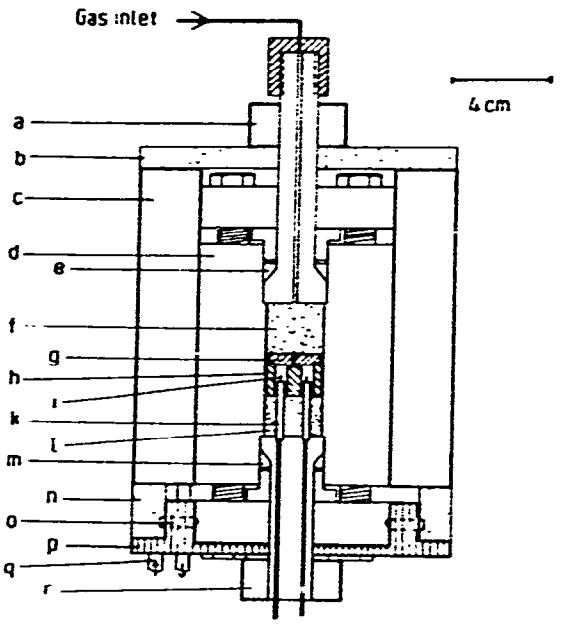

Fig. 5.16. High pressure DTA cell of Kuballa and Schneider[91]. a, r = coolers; b, n = pyrophillite insulating disk; c = heating block; d = high pressure vessel; e, m = copper seals; f, l = ZrO_2 blocks; g = copper shield; h = calorimeter block; i = thermocouple; k = corundum capillary; o = fastening screw; p = support; q = in- and outlet of refrigerant.

Other high pressure DTA systems have been described[92-95], while Locke[96] discussed the chemical applications of the Stone high pressure DTA system.

5.3.3. Miscellaneous DTA instruments

Modifications to commercial DTA instruments for the measurement of vapor pressures and heats of vaporization have been described[97,98]. Low temperature DTA instrumentation has been reviewed by Bohon[99] and Redfern[100]. A DTA instrument, using high frequency electrical field heating, has been described[101]. Fujino et al.[102] described an apparatus in which the thermal conductivity of a sample may be obtained from the DTA curve. Micro DTA systems have been described[103,108] as well as DTA measurements in a fluidized bed[104].

High temperature DTA instruments have been discussed by numerous investigators. Šesták et al.[105] described an apparatus which could be used up to a maximum temperature of 1300°C while an ultra-high temperature system was discussed by Rupert[106]. The derivative capability of the latter is a unique and useful feature of the apparatus.

A DTA apparatus which permits agitation of the sample has been described by Gilpatrick et al.[107]. Such an apparatus was found to be useful for phase studies in molten salt systems. A miniature DTA system, designed for extra-terrestrial explorations, has been described by Bollin[109]. A DTA instrument in which measurements are made in an isothermal mode in five samples has been discussed by Burr[110].

Wendlandt and Bradley[111] have described an automated DTA instrument in which samples are automatically introduced into the furnace, heated to a preselected temperature limit, and then removed. After the furnace has been cooled back to room temperature, the cycle is repeated.

5.4. Differential scanning calorimetry

There has been some confusion concerning the use of the term "differential scanning calorimetry" (DSC). Two industrial firms use the term to describe their instruments, yet each type is based on a different principle of operation. Several DSC instruments are based on the principles of DTA rather than that of a dynamic calorimeter. A distinction between the DSC instruments can be made by examination of the calorimetric response or calibration curve. For DTA type instruments, the calorimetric response of the instrument decreases with an increase in temperature, i.e., it requires more calories per unit peak area at elevated temperature. For true DSC instruments, the calorimetric response is invariant with temperature. Thus, in the latter type instruments, only one calibration temperature is required, while in the former, a series of calibration points is needed over the temperature range of interest. There are numerous disadvantages of the DTA type over those of DSC instrument for quantitative calorimetry but they will not be discussed here. Also, generally speaking, true DSC type instruments are more sophisticated electronically than the DTA type instruments.

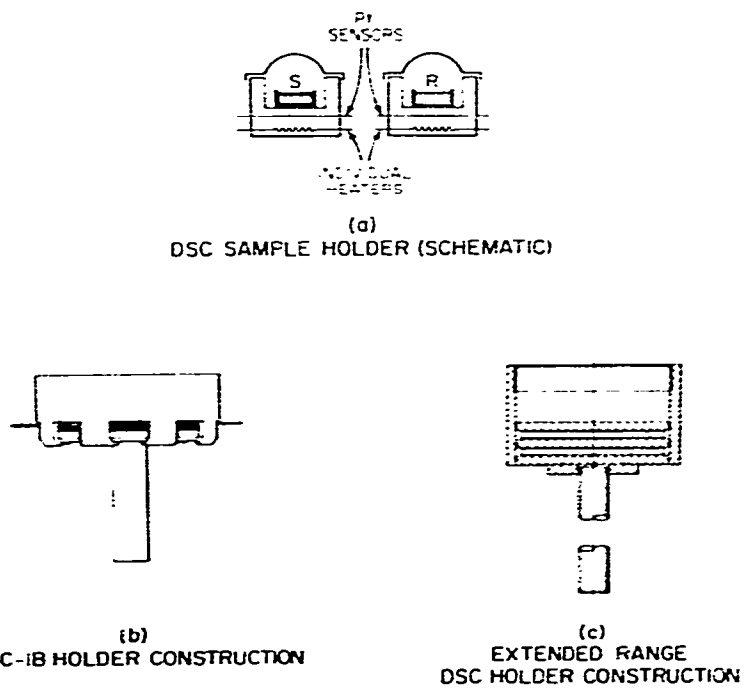

Fig. 5.17. Sample holder construction used in the Perkin–Elmer DSC instruments[115].

Perhaps the most widely used true DSC instrument has been the Perkin-Elmer differential scanning calorimeter. Model DSC-1, introduced in 1963[112,113]. Recently introduced[114–116], the Model DSC-2, which has an extended temperature range to 725 C, improved base line repeatability and linearity, and a higher calorimetric sensitivity. A comparison[115] of the sample holders used in the DSC-1, DSC-1B, and DSC-2 instruments is shown in Fig. 5.17. In the DSC-1 cell, the sample and reference holder consisted of a stainless steel cup and support, a platinum wire sensor, an etched Nichrome heater, and other thermal parts. All of these components were mechanically crimped together in a very tight sandwich. This sample holder operated well over the temperature range of −125 to 500 C. In the DSC-2 sample holder, the materials of construction used are a platinum–iridium alloy for the body and structured members of the holder, a platinum wire for both the heater and sensor, and α-alumina for electrical insulation. All parts of the holder are spot-welded together.

Various sample holders have been described for the Perkin-Elmer DSC instrument. A sealed metal cell with a removable screw-on cap has been described by Freeberg and Alleman[117]. Metals used were brass, stainless steel, and aluminum. Wendlandt[118] described a capillary tube sample holder which used 1.6–1.8 mm diameter glass capillary tubes. The tubes were contained in an aluminum holder which sat in the sample and reference cells of the calorimeter. Sample holders for measuring the vapor pressure of a liquid[119] as well as for heats of mixing[120] have been described. Enclosure of the sample holder chamber in a vacuum chamber has been described by Morie et al.[121].

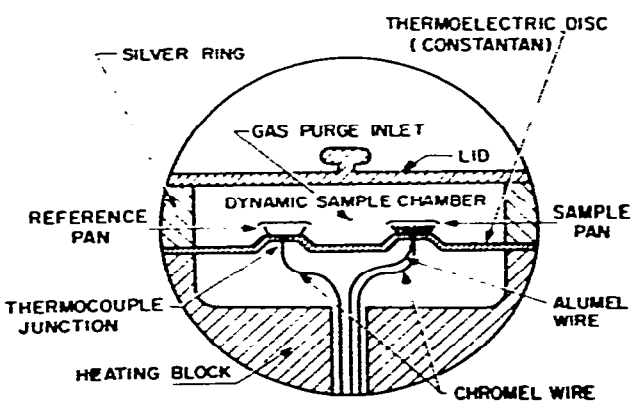

Fig. 5.18. The DuPont DSC cell[122].

A discussion of the theory and operational characteristics of the DuPont DSC cell has been given by Baxter[122]. The DSC cell, as shown in Fig. 5.18, is based on a thermoelectric disc made of constantan which serves as the major path of heat transfer to and from the sample and also as one-half of the ΔT measuring thermocouples. A chromel wire is connected to each platform, thus forming the Chromel–constantan differential thermocouple. Temperature range of the instrument is −150 to 600 °C. The utility of this DSC cell has been extended by its enclosure in a

pressure chamber capable of operation to 67 atm. This high pressure system has been described by Levy et al.[123].

A new DSC cell, based on the DTA principle (as is the DuPont DSC cell previously described), has been described by David[124]. The calorimeter cell, as shown in Fig. 5.19, contains a differential thermocouple of a new thin form design

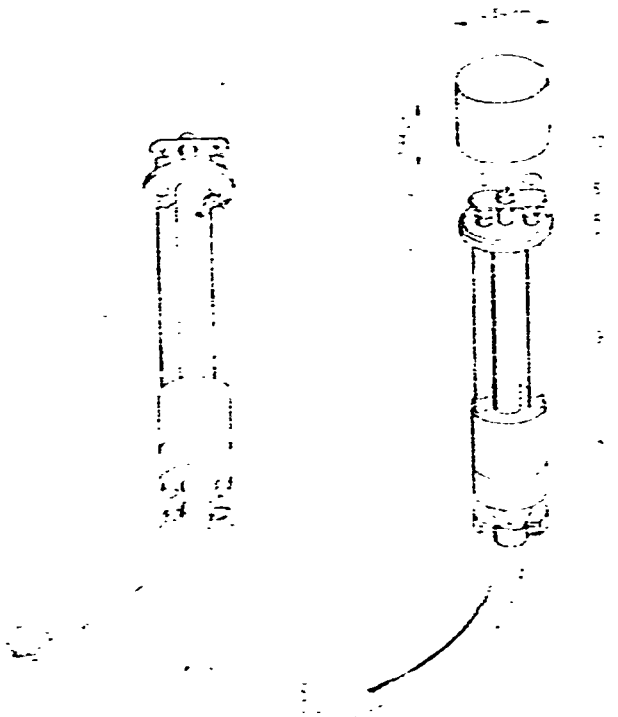

Fig. 5.19. DSC cell by David[124]. 1 = thermocouple for x-axis or system temperature readout; 2 = limit switch thermocouple; 3 = programming or furnace thermocouple; 4 = dynamic gas port entry; 5 = dynamic gas port exit; 6 = sample side of differential thermocouple; 7 = reference side of differential thermocouple; 8 = ceramic thermal insulator; 9 = ceramic support rods; 10 = sample pans.

that is isolated from the cell wall and bottom to provide greater sensitivity. This thermocouple consists of a sheet of negative Platinel II type thermocouple alloy coupled to a positive Platinel II alloy. Flat shallow containers are employed for the sample and reference materials. Two additional thermocouples are used for measuring the temperature of the cell and are used for the furnace programmer, limit switch, and temperature readout. The maximum temperature of the cell is 1000 °C.

A large number of other dynamic calorimeters have been described in the literature, many of which have been described in an excellent review by Wilhoit[125].

Schematic diagrams of the Deltatherm dynamic adiabatic calorimeter, as discussed by Dosch and Wendlandt[126], are shown in Fig. 5.20. As illustrated in Fig. 5.20A, the temperature difference between the sample and adiabatic enclosure is detected by the differential thermocouple, TC1. This temperature difference then

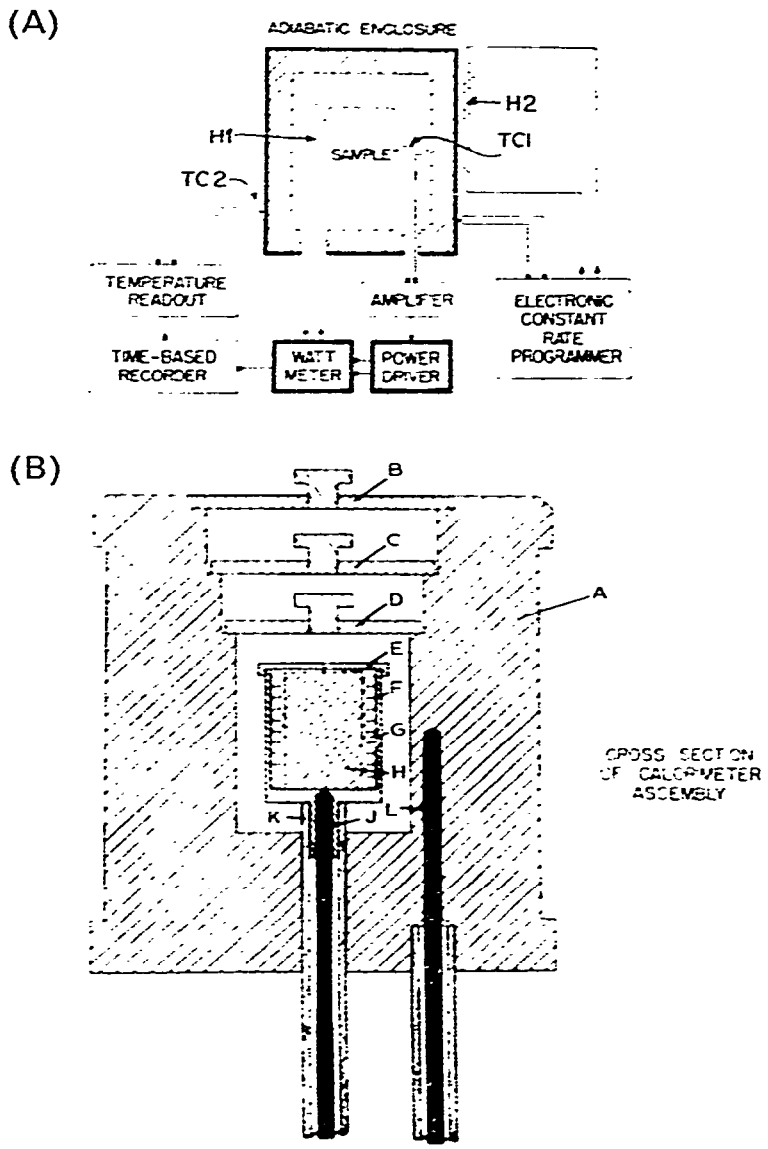

Fig. 5.20. Deltatherm calorimeter[126]. (A) Block diagram of entire system; (B) Cross section of calorimeter, where A = copper block; B, C, and D = copper covers; E = sample chamber cover; F = sample chamber; G = heater; H = sample; J = thermocouple; K = ceramic support; L = thermocouple.

controls the output of the power driver which applies power to heater H1. Power input to the heater is measured by a Hall effect multiplier watt-meter. The calorimeter assembly (Fig. 5.20B) is mounted on a ceramic pillar and consists of a massive copper block, A, enclosed by copper covers B, C, and D. The sample chamber, F, and its cover are made of silver and thermally isolated from the block. Sheathed thermocouples, J and L, are used for temperature detection. Samples may be in the form of solid blocks, powders or liquids.

Other calorimeters described include a microcalorimeter[127] similar to the Calvet instrument[128]; a spherical high temperature adiabatic calorimeter[129]; high temperature differential calorimeters[130–133]; and others[134–137].

5.5. *Gas evolution detection and/or analysis*

The simultaneous detection or analysis of the evolved gaseous products adds another dimension to thermal analysis investigations. The evolved gases can be detected (GED) or analyzed (GEA) for composition thus aiding in the interpretation of DTA or TG curves. Gas evolution detection is often most useful for the interpretation of DTA curves; solid → solid transitions can easily be distinguished from solid → solid + gas type reactions and so on. Physicochemical data, such as heat of vaporization, heat of reaction, kinetics, and so forth, can also be obtained by this technique.

The principles and instrumentation of gas evolution detection and analysis have been reviewed by various textbooks[3,66,138,139]. As with the other techniques discussed in this chapter, only the more recent developments in instrumentation will be described here.

The combination of GED and GEA with a thermobalance has been discussed in section 5.2.4. Using the Derivatograph, Paulik et al.[140–144] described a thermo-gas-titrimetric (TGT) technique and also derivative thermo-gas-titrimetry (DTGT).

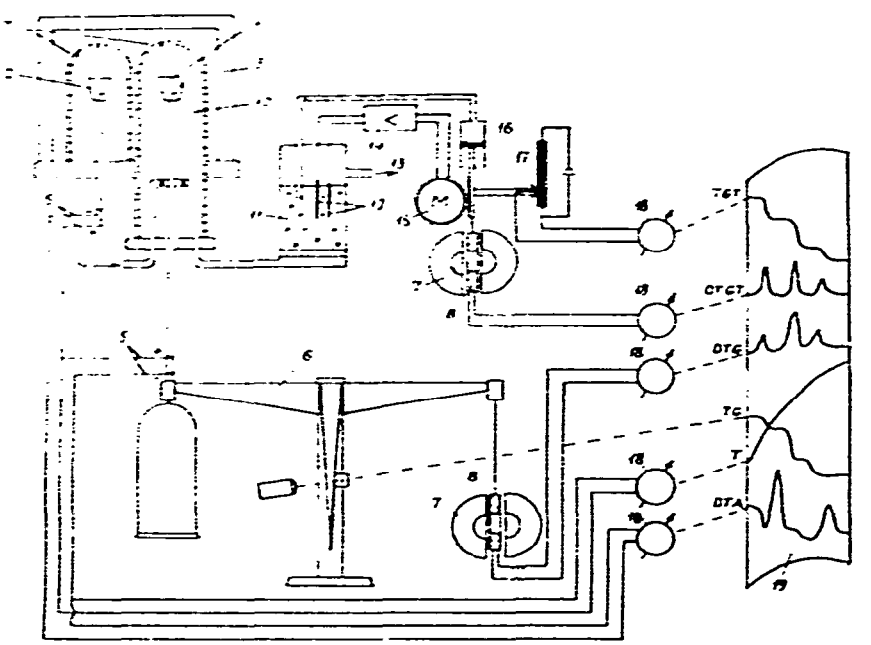

Fig. 5.21. TGT and DTGT apparatus as used by Paulik and Paulik[141]. 1 = sample; 2 = inert substance; 3 = furnace; 4 = quartz bulbs; 5 = thermocouples; 6 = balance; 7 = permanent magnet; 8 = coil; 9 = inlet of inert gas; 10 = gas outlet; 11 = absorber; 12 = electrodes; 13 = exhaust; 14 = amplifier; 15 = motor of the automatic burette; 16 = automatic burette; 17 = potentiometer; 18 = galvanometers; 19 = photopaper.

The apparatus employed in this technique is shown in Fig. 5.21. An inert carrier gas is used to flush the gaseous decomposition products from the furnace chamber into an aqueous absorbing solution. As the pH of the absorbing solution changes, an automatic buret adds titrant to the solution restoring it to its original value. A slide contact of a potentiometer moves with the piston of the buret, and a galvanometer coupled to the potentiometer records the TGT and DTGT curves. A comparison of the TGT and TG curves of $[Cu(NH_3)_4]SO_4 \cdot H_2O$ is shown in Fig. 5.22. The first step, the loss of one mole of water, is followed by the loss of two moles of ammonia and then two steps of one mole of ammonia each.

The detection of gaseous decomposition products by infrared spectroscopy has been described by Kiss[145,146]. Evolved gases from a Chevenard thermobalance are flushed into an infrared cell where the concentrations of ammonia and water were determined.

Changes of pressure in a TG system due to the evolution of gaseous decomposition products has been named thermobarogravimetric analysis (TBGA)[147,148]. Maycock and Pai Verneker[148] described a system consisting of a Mettler thermobalance coupled to a Baratron differential pressure gauge.

Pressure changes within a system can be measured with various types of detectors: Turcotte et al.[149] used a capacitance micrometer while Guenot et al.[150] used a differential pressure gauge. Detection and/or analysis of evolved gases with a thermal conductivity detector[151–153], gas chromatograph[152,154], mass spectrometer[154,155], specific gas detectors (e.g., CO_2 and SO_2)[156], and condensation nuclei, have been discussed[157–159].

The combination of thermal analysis–flame ionization detection (TAFID) has been described by Eggertsen et al.[160–162] for the precise measurement of vaporization patterns of organic compounds. The basic system, as shown in Fig. 5.23, consists of a small furnace connected to a flame ionization detector. Also included is a gas-flow scheme to supply carrier gas (usually N_2), hydrogen and air for the flame detector, air

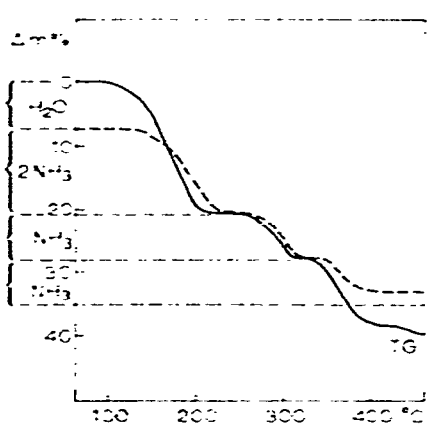

Fig. 5.22. TG and TGT curves of $[Cu(NH_3)_4]SO_4 \cdot H_2O$[143]. (———) TG curve; (– – –) TGT curve.

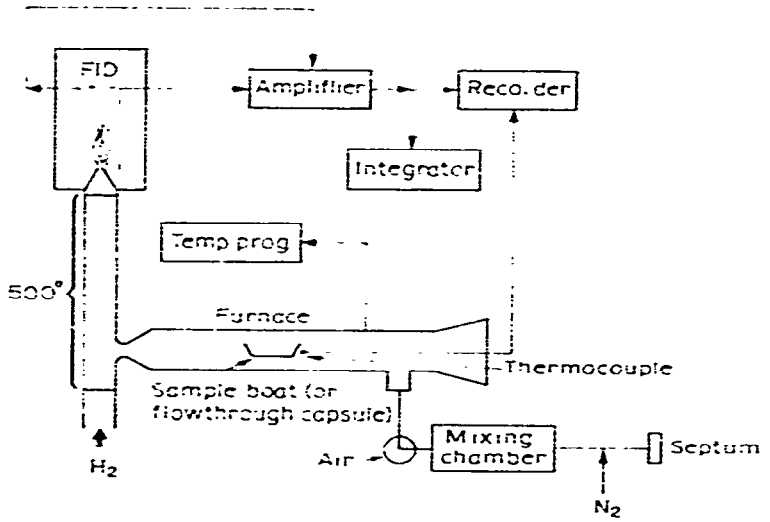

Fig. 5.23. Schematic diagram of TAFID system of Eggertsen and Stross[162].

for burning out residues in the furnace, and air for rapid cooling of the furnace. The sample boat is made of aluminum, platinum, or gold and is held in a stainless-steel wire frame attached to a sheathed thermocouple. The probe is so constructed that the supporting rod can slide through the joint at the inlet of the furnace. Various other probes have been described, each for a specific purpose, e.g., vapor pressure determination, etc. The lowest limit of detection of the detector is 1×10^{-4} μg of carbon per min. Temperature range of the instrument is 25 to 500°C.

Bollin[109] described a miniature DTA–EGA apparatus for a Martian landed capsule. Such an application should have direct application to laboratory type chemical problems.

5.6. Electrical conductivity

The measurement of the electrical conductivity of a sample as a function of temperature has been described by a number of investigators. This technique has been called electrothermal analysis (ETA)[163] or amperometric thermal analysis (ATA)[164].

The apparatus used by David[164] for simultaneous DTA–ATA measurements is shown in Fig. 5.24. One platinum electrode (H) was a 20 gauge platinum wire while the other consisted of a platinum lead attached to a small stainless steel cylinder which was plated with platinum (F). The small platinized cylinder received the same type of sample cup that was utilized in the ring-type thermocouples, and made contact with the edge of the cylindrical receiver by virtue of the sample cup lip. A movable electrode system was used to maintain continuous contact with the sample during first-order phase transformations in which a reduction in bulk volume frequently occurs. A suitable d.c. voltage from 1 to 1000 V was applied to the sample and the current flow through the system was measured by an electrometer in series with the

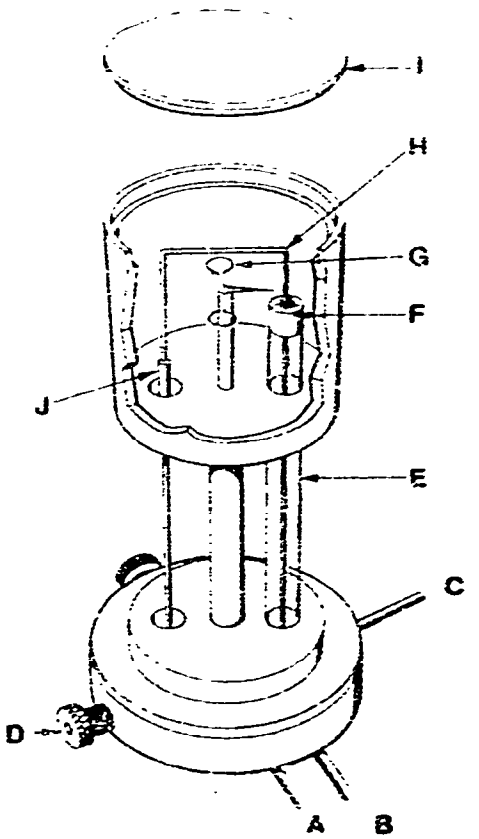

Fig. 5.24. DTA–ATA sample holder used by David[164]. A = electrometer input lead; B = negative voltage input lead; C = thermocouple leads; D = cooling water connectors; E = pyrex capillary voltage insulator; F = sample pan container; G = differential thermocouple; H = platinum electrode; I = sample holder cover; J = platinum electrode coupler.

voltage source. Loss of evolved water in the dehydrations of $CuSO_4 \cdot 5H_2O$ was followed by this technique as well as the fusion behavior of KNO_3 and polymeric materials[164].

Wendlandt[165] used electrical conductivity measurements to detect the quadruple points in various metal salt hydrate systems. Quadruple points can frequently be detected by DTA, as was shown in the case of $CuSO_4 \cdot 5H_2O$[166]. The first endothermic shoulder peak was related to the coexistence of four phases in the system: $CuSO_4 \cdot 5H_2O$, $CuSO_4 \cdot 3H_2O$, $H_2O(l)$, and $H_2O(g)$.

The electrical conductivity apparatus used by Wendlandt[165] is shown in Fig. 5.25. The apparatus consisted of a recording micro-micro-ammeter, a X–Y recorder, a power supply in the 3–25 V d.c. range, a sample holder and electrode probe, and a metallic block furnace whose temperature rise was controlled by a programmer. Powdered samples of the metal salt hydrates were contained in Pyrex glass tubes, 5 mm in diameter by 50 mm in length.

A typical electrical conductivity (EC) curve of $CuSO_4 \cdot 5H_2O$ is shown in Fig. 5.26. The EC curve consisted of a single peak, due to the liberation of a liquid

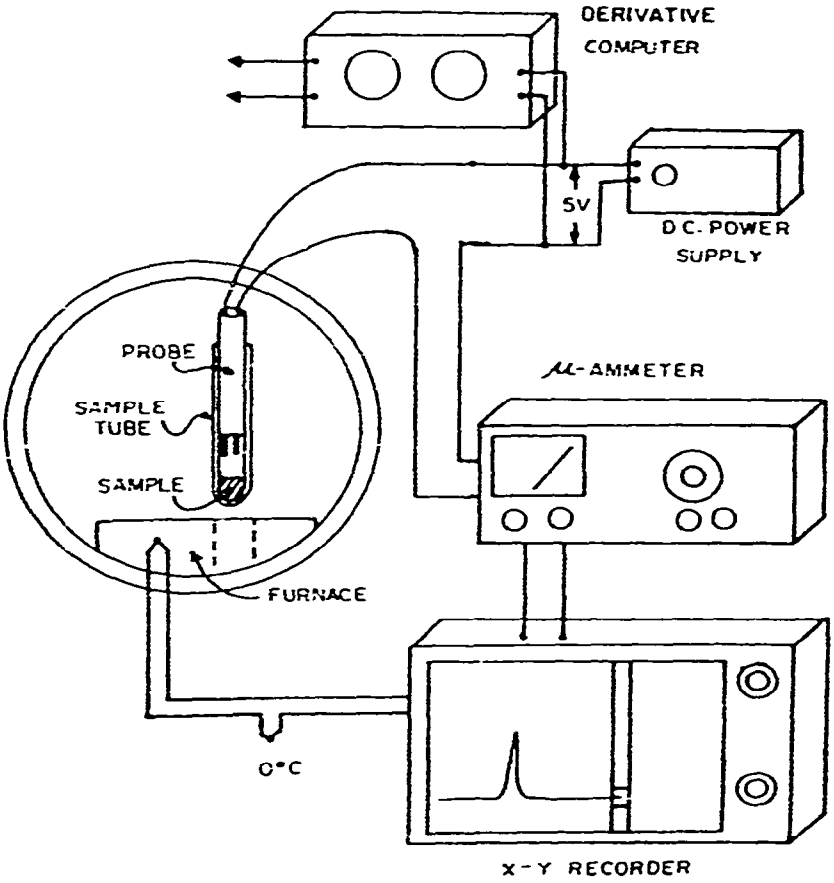

Fig. 5.25. Electrical conductivity apparatus used by Wendlandt[165].

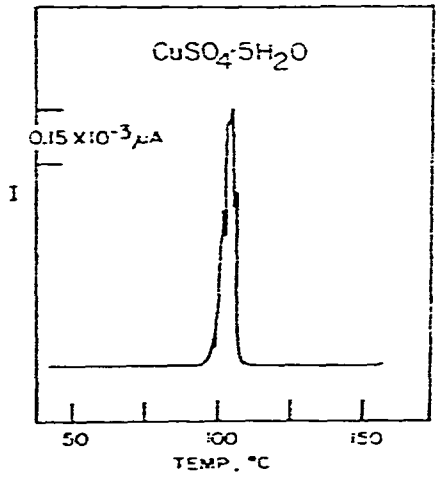

Fig. 5.26. Electrical conductivity curve of $CuSO_4 \cdot 5H_2O$ (ref. 165).

water phase from the hydrate, which began at a temperature of 97 °C. No other liquid phases were detected in the system in the temperature range investigated. Similar results were obtained for $BaCl_2 \cdot 2H_2O$ and $BaBr_2 \cdot 2H_2O$.

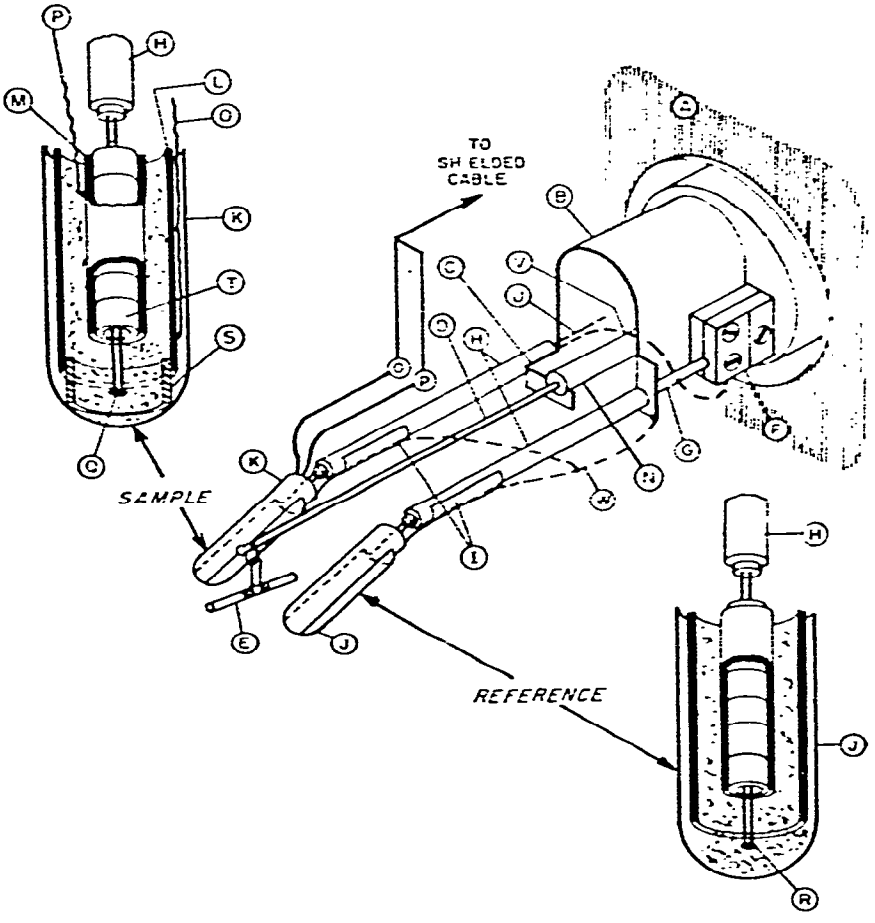

Fig. 5.27. Apparatus used by Chiu[163] for parallel TG–DTG–DTA and ETA measurements. A = balance housing; B = balance beam sheath; C = beam stop; D = quartz beam; E = sample container; F = thermocouple block; G = sample measuring thermocouple; H = ceramic tubing; I = platinum jacket; J = reference quartz tube; K = sample quartz tube; L = outer platinum electrode; M = center platinum electrode; N = cold beam member; O, P = platinum lead wires; Q = sample thermocouple junction; R = reference thermocouple junction; S = spacer; T = ceramic insulation; U, V = sample thermocouple wires; W = platinum grounding wire.

Chiu[163,167] used electrothermal analysis as a parallel measurement with TG, DTG, and DTA. The sample handling system is shown in Fig. 5.27. One electrode (M) in the sample holder is a 0.003 in thick piece of platinum foil wrapped around the ceramic insulation (T) of the sample thermocouple (Q). The other electrode (L) is made from platinum foil in the form of a cylinder to fit the inside of the quartz tube (K). The sample is packed tightly between the two electrodes; spacer (S), located at the bottom of the tube is used to prevent accidental shorting of the electrodes. The

current flowing through the system, under an applied d.c. potential of 1–2 V, is detected with an electrometer and recorded on the Y-axis of an X–Y recorder. Sample currents from 10^{-10} to 10^{-5} amp, in five decades, were recorded.

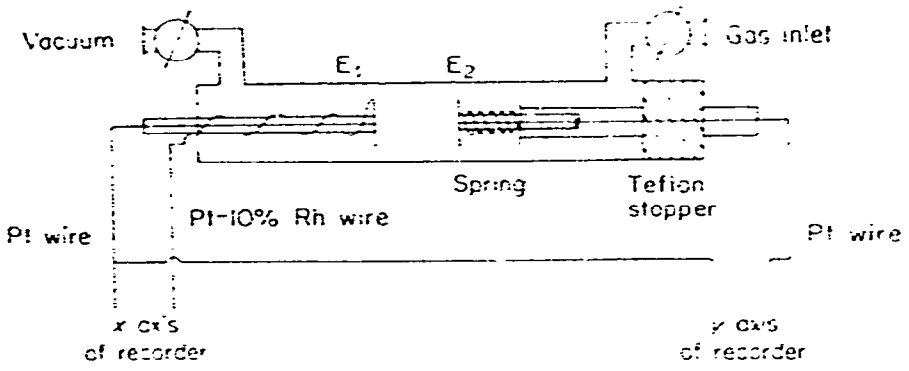

Fig. 5.28. Electrical conductivity apparatus of Rudloff and Freeman[168].

Rudloff and Freeman[168] used the EC apparatus illustrated in Fig. 5.28 to study the conductivity of several metal oxides. Electrode E_1, inside of a flow tube of Vycor glass, was mounted on a glass disc that is fused to a sturdy glass capillary tube fixed at one side of the flow tube. Electrode E_2 is fixed on a similar disc-capillary combination. A spring provides adequate pressure of the electrodes to the single crystal or powder pellets for good electrical contact. The flow tube can be placed into a heated tube furnace. During operation, the entire system must be carefully shielded to prevent noise pickup from the surroundings.

An apparatus for simultaneous ETA and dilatometry has been described by Judd and Pope[169]. It consisted of a thermal aluminous porcelain 525 tube mounted horizontally in a Kanthal wound tube furnace capable of operation up to 1250 C. The tube is reduced to a narrow neck at one end to which the vacuum line is connected. The other end of the tube is fixed to a metal bracket via two O-rings, giving a vacuum-tight connection. A spacer keeps the compacted sample in a fixed position near the center of the furnace. Electrical contact with the sample is made by means of two platinum disc electrodes pressed against the opposing faces.

Carroll and Mangravite[170] described an apparatus in which simultaneous EC and DSC measurements could be made on the same sample. They referred to the technique as simultaneous scanning calorimetry and conductivity (SSCC).

5.7. High temperature microscopy

The most important applications of high temperature microscopy, according to McCrone[171], are characterization and identification of pure compounds, determination of purity, analysis of binary mixtures, determination of composition diagram for binary and ternary systems, elucidations of phase diagrams, poly-

morphism, crystal growth kinetics, and studies of crystal-lattice strain. These applications have been discussed in detail in well known textbooks[172,173] as well as the instrumentation employed. The Kofler hot stage[173] has been employed for high temperature studies since the 1930's and a commercial version appeared in 1940. Introduced in 1968, the Mettler Model FP-2 hot stage, as shown in Fig. 5.29, has been

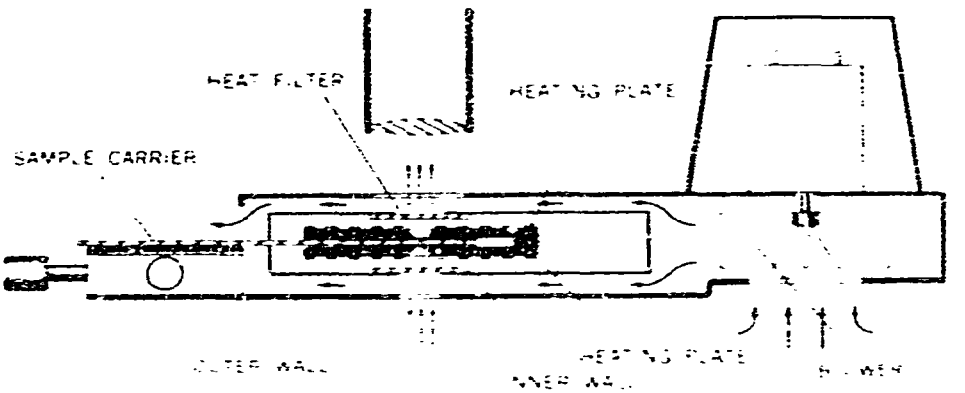

Fig. 5.29. Mettler Model FP-2 microscope hot stage.

widely used. This apparatus made possible for the first time the measurement of the sample temperature without embedding the temperature detection device in the sample. The temperature can be controlled within ±0.02°C, making equilibrium melting point determinations a simple matter. Applications of the Mettler hot stage have been reviewed by Vaughan[174], and van Tets and Wiedemann[175].

Various hot stage furnaces for use up to a maximum temperature of 2000 C have been described[176,177] while Bruckner and Heide[178] discussed in detail some applications of the Zeiss hot stage.

An automatic thermomicroscopy apparatus was used by Faubion[179] to study polymorphic transitions of high explosive compounds. This system was based on an apparatus previously described by Kolb et al.[180]. Other similar instruments have been described[174,181].

A hot stage microscope which can also be used as a micro-DTA instrument has been described by Sommer and co-workers[182–185]. The apparatus is based upon the use of two opposed, viewable, thermocouple microfurnaces which used samples of less than 1 mg and which may be rapidly quenched or heated. A maximum temperature of 1800 C is attained although with suitable thermocouples, the maximum working temperature may be increased to 2500 C.

The apparatus, as shown in Fig. 5.30, uses a triple function thermocouple junction. It incorporates the simultaneous heating and measurement of temperature, alternate heating and measurement of temperature, and half-cycle heating incorporating the use of semi-conductors. This system can also be applied to the study of rate-dependent crystallization processes in oxide melts as well as for the study of non-equilibrium, high-rate thermal changes.

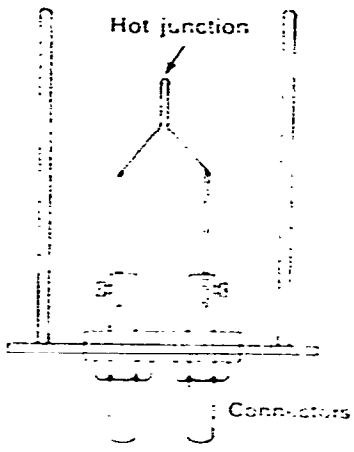

Fig. 5.30. Cell and thermocouple assembly used by Sommer et al.[185].

A balanced temperature thermal analysis apparatus was also described[185]. In this method, both thermocouples with their respective samples are kept at the sample temperature (the temperature being controlled by the temperature programmer) and the electrical power that has to be supplied to achieve this is determined. This system removes the criticism often used in quantitative DTA that during reactions in the sample, the rate of change of temperature cannot be controlled.

5.8. Emanation thermal analysis

The technique of emanation thermal analysis (ETA) is based on the introduction of inert radioactive gases into a solid and the measurement of their subsequent liberation from the substance as it is heated[186–188]. Release of the radioactive gas makes possible the monitoring of various types of changes taking place during the thermal cycle. These include chemical reactions such as dehydration, thermal dissociation, and synthesis; polymorphic transformations, melting, conversion of metastable amorphous structures into crystalline compounds and changes in the concentrations of lattice defects. The ETA technique possesses several advantages over conventional TG and DTA. Under dynamic conditions, it permits the study of structural changes of compounds even when these changes are not related to a thermal effect (e.g., second order phase transformations). In other cases, when finely crystalline or amorphous phases are formed, ETA is more sensitive than X-ray methods.

The ETA apparatus[188], which also permits the recording of the DTA and dilatometric curves concurrently, is shown in Figs. 5.31 and 5.32. A labelled sample (generally 100 mg), a DTA reference material (Al_2O_3), and a sample for dilatometric measurements are placed in the heated chamber. Temperature measurement is by thermocouples embedded directly into the samples. A heating rate of 8 to 10°C/min is normally used since this is an optimum rate for DTA as well as ETA measurements.

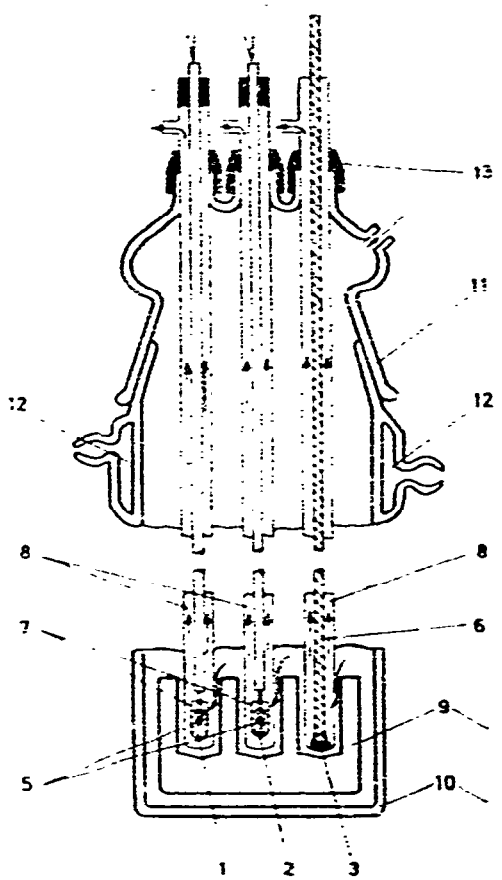

Fig. 5.31. Reaction chamber for concurrent ETA, DTA, and dilatometric measurements (after Balek)[188]. 1 = activated sample; 2 = DTA standard; 3 = dilatometer sample; 5 = composite thermocouple; 6 = quartz dilatometer rod; 7 = quartz vessels; 8 = supporting pipes; 9 = metal block; 10 = quartz outer vessel; 11 = ground glass joint; 12 = coolant tube; 13 = gas tight seals.

The radioactive gas released from the solid sample is carried by a carrier gas stream which flows at a constant rate into the cells for gas radioactivity measurements (Fig. 5.32). The apparatus simultaneously registers α-activity of radon and the β-activity of xenon introduced by ion bombardment. An ETA curve is recorded together with the DTA and dilatometric curves using a multi-point recorder.

In the ETA method, the number of atoms emanated from a small crystallite can be written as the sum of two terms[189]:

$$E = E_r + E_d, \text{ or}$$

$$E = \left(\frac{r_0 S}{4m}\rho\right) + \left(\frac{D_0}{\lambda}\right)^{1/2} \frac{S}{m}\rho \exp\left(-\frac{Q}{2RT}\right)$$

where E_r is the emanation released due to the recoiled emanation atoms, E_d the diffusion part of the reduced emanation atoms, r_0 the range of recoiling atoms, S the

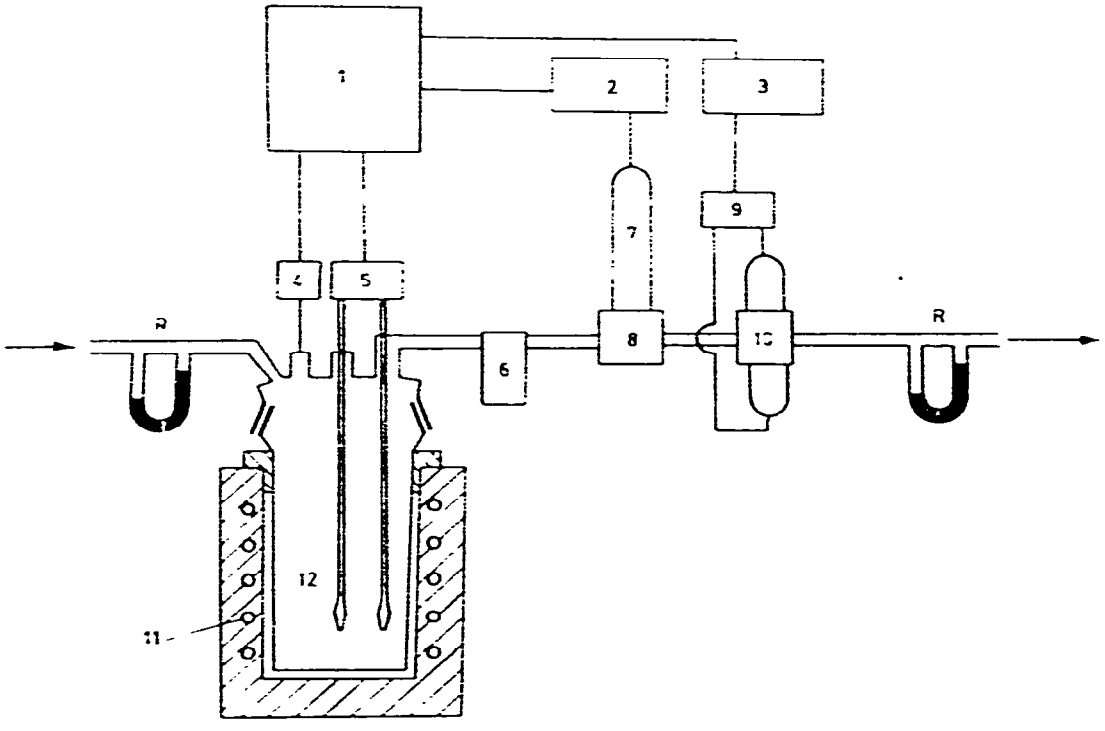

Fig. 5.32. ETA apparatus[185]. 1 = electronic potentiometer; 2 = alpha count integrator; 3 = beta count integrator; 4 = dilatometer pickup; 5 = thermocouple; 6 = gas dryer; 7 = photomultiplier; 8 = scintillation chamber; 9 = cathode repeater; 10 = β emission measurement chamber; 11 = electric heater; 12 = quartz reaction vessel; R = rheometer.

specific surface, m the crystalline mass, D_0 the pre-exponentional term in the expression

$$D = D_0 \exp(-Q/RT)$$

where D is the diffusion constant, Q the activation energy of diffusion of the emanation in the solid, R the gas constant, ρ the density, λ the decay constant of emanation, and T the absolute temperature.

The temperature dependence of the rate of emanation release from Fe_2O_3 is shown in Fig. 5.33a. Alternatively, a semilogarithmic curve of the form of $E_d = f(1/T)$ may be constructed, as shown in Fig. 5.33b; the quantity E_d being evaluated from E (emanation power at the relevant temperature) and E_r (value of E measured at room temperature). In Fig. 5.33b, two slopes may be seen in the curve. A low temperature section with a low value of $2 \log E_d / 2T$ and a high temperature section with a larger value of $2 \log E_d / 2T$. The discontinuity on the curve lies at 693 °C, i.e., 0.53 of the absolute melting point of Fe_2O_3. With other crystalline, powdered inorganic substances, the discontinuity on the curve corresponds to 0.5 to 0.6 of their absolute melting point. This temperature is related to the beginning of sufficiently intensive motion of atoms or ions in the crystal lattice to cause an effective diffusion rate in the solid. Based on the classical emanation method, it is therefore possible to determine

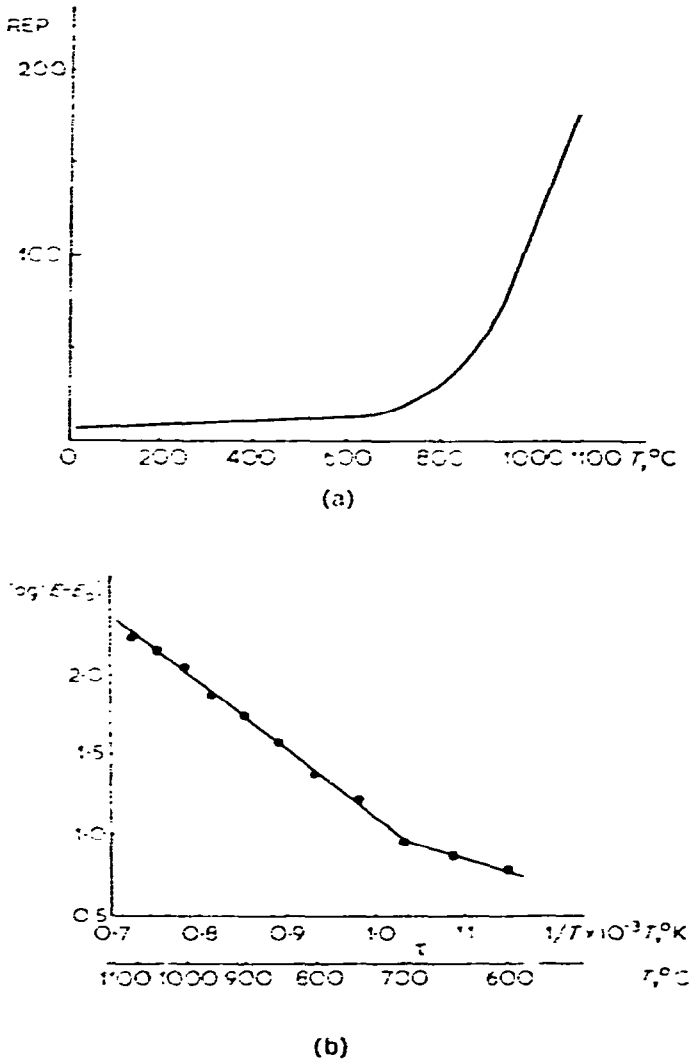

Fig. 5.33. Emanation curve of Fe_2O_3: (a) in $E = f(T)$ coordinates; and (b) in $\log(E - E_r) = f(1/T)$ coordinates. E_r being the value of E at room temperature.

this temperature range, which is of great practical importance since above this approximate temperature it is possible that solid-state reactions can occur by diffusion mechanisms. The slope of individual sections of the curve can be used to determine the activation energy of the emanation process in a solid for a specified temperature range. The E of radon-diffusion in Fe_2O_3 was evaluated as $Q = 15 \pm 3$ kcal mole^{-1} in the range of 600–700 C and $Q = 40 \pm 5$ kcal mole^{-1} in the range of 850–1100 C.

The ETA and DTA curves[186] of $Th(C_2O_4)_2 \cdot 6H_2O$ are illustrated in Fig. 5.34. The ETA curve reveals three processes taking place: (1) Stepwise dehydration in the temperature range of 40–220 C; the DTA curve shows only two endothermic peaks in this range for the transitions of $6H_2O \rightarrow 2H_2O$ and $2H_2O \rightarrow 1H_2O$; (2) the flat peak in the 300–400 C range corresponds to decomposition of $Th(C_2O_4)_2 \cdot H_2O$:

(3) the last peak, at 400–500 °C, is due to the conversion of amorphous ThO_2 to crystalline. The curve of the rate of release of xenon which had been incorporated into the sample by ionic bombardment fully confirms the reaction sequence indicated by the ETA curve.

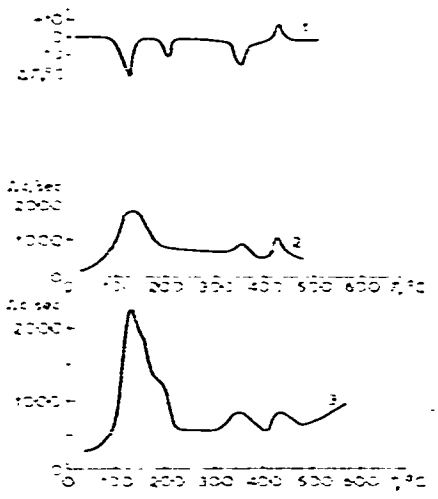

Fig. 5.34. The thermal decomposition of $Th(C_2O_4)_2 \cdot 6H_2O$. (1) DTA curve; (2) temperature dependence of xenon release; (3) ETA curve[186].

5.9. Thermomagnetic analysis

The measurement of the magnetic susceptibility of a compound as a function of temperature is frequently useful for the detection of changes of oxidation state, reduction and oxidation reactions, ferromagnetic and antiferromagnetic behavior, and so on. Without temperature-dependent studies the prediction of the number of unpaired electrons, oxidation state, and stereochemistry of magnetically concentrated systems must be suspect[190].

Numerous instruments permitting variable temperature control of the sample chamber have been described. One of the more recent instruments employs the variable temperature accessories for a nmr or epr spectrometer[190] to obtain measurements by either the Gouy or Faraday methods. Mulay and Keys[191] described a helical-spring microbalance for Faraday type magnetic susceptibility as well as for adsorption and TG measurements. Measurements of the dehydration of $CuSO_4 \cdot 5H_2O$, as shown by the data in Table 5.2, illustrate the application of the balance for TG and thermomagnetic analysis (TMA). Four moles of water were evolved between 25 and 100 °C under a system pressure of ca. 10^{-6} torr. The change in susceptibility is due not only to the loss of water molecules but also to a change in paramagnetism of the sample. The latter factor is easily accounted for by calculating theoretically the susceptibility for $CuSO_4 \cdot 5H_2O$ at 100 °C, on the basis of the Curie–

TABLE 5.2

TG AND TMA DATA FOR $CuSO_4 \cdot 5H_2O$[191]

Temp., °C	*Expected formula*	X_g ($\times 10^{-6}$ c.g.s. units)	X_m ($\times 10^{-6}$ c.g.s. units)	ΔX_m ($\times 10^{-6}$ c.g.s. units)
25	$CuSO_4 \cdot 5H_2O$	5.860	1129.6	
100	$CuSO_4 \cdot H_2O$	6.632	1178.4	−49[a]
($p = 10^{-6}$ torr)				

[a] Corresponds to 4 moles of water if $X_m(H_2O) = -12.9 \times 10^{-6}$ c.g.s. units.

Weiss law. Another application of the apparatus was to study the adsorption of oxygen on γ-alumina and measurement of the changes in magnetic susceptibility during adsorption. Measurements indicate the formation of a dimeric O_4 species with a very small magnetic susceptibility.

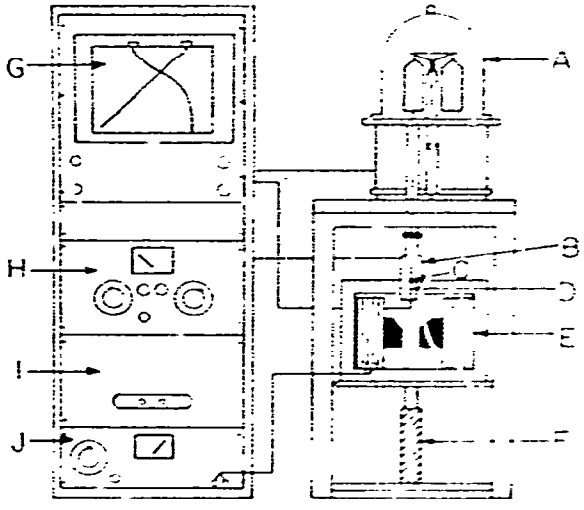

Fig. 5.35. TG–TMA apparatus of Simmons and Wendlandt[192]. A = Ainsworth semi-micro recording balance; B = tube furnace; C = sample container; D = furnace thermocouple; E = electromagnet; F = hydraulic piston; G = two-pen recorder; H = furnace temperature programmer; I = voltage regulator; J = magnet power supply.

Simmons and Wendlandt[192] have described a Faraday type instrument in which TG and TMA measurements can be obtained from room temperature to 500 °C. The apparatus is illustrated in Fig. 5.35. A two channel recorder was employed in which one channel recorded the temperature, the other the TG curve. Superimposed on the TG curve were the deflections of the sample caused by the introduction of the magnetic field about the sample at periodic intervals. The TG–TMA curve of $[Co(NH_3)_6]Cl_3$ is shown in Fig. 5.36. A more useful parameter of this system is the mole percent of cobalt(III) reduced, as a function of temperature, as is

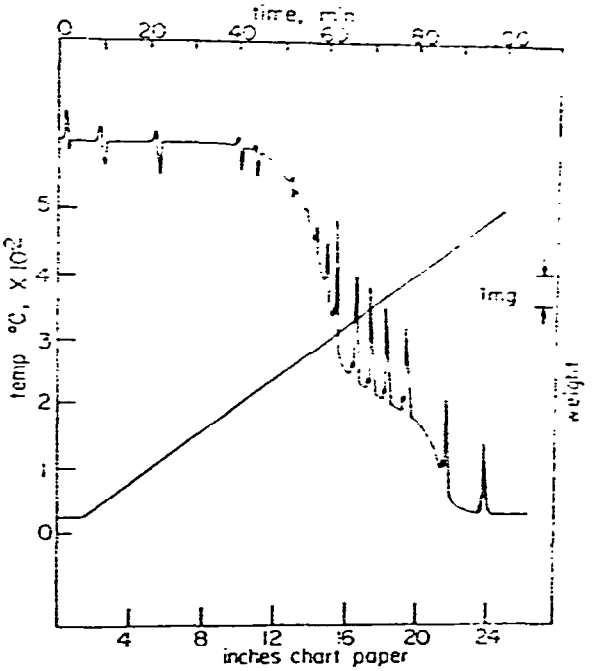

Fig. 5.36. TG–TMA curve of $[Co(NH_3)_6]Cl_3$[192].

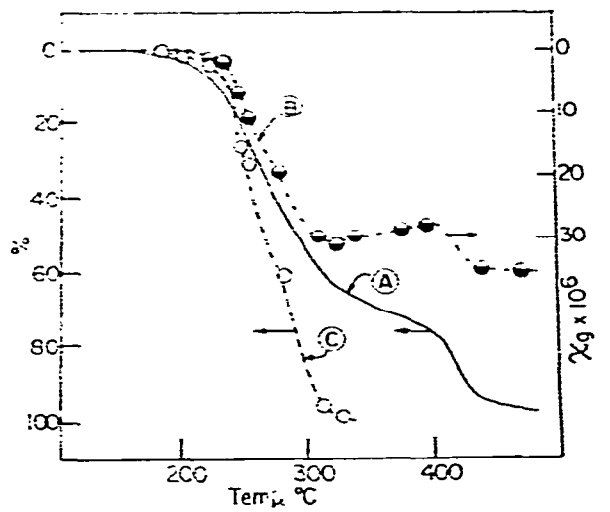

Fig. 5.37. TG, mass susceptibility and molar percent reduction of $[Co(NH_3)_6]Cl_3$. (A) TG curve; (B) mass susceptibility curve; and (C) mole percent cobalt (III) reduced curve.

shown in Fig. 5.37. This parameter is calculated from the equation[192]:

$$\text{mole percent reduced} = 100\,\frac{\left[\left(\frac{\Delta m-\Delta m_c}{\Delta m_s-\Delta m_c}\right) m_s X_s (2.84)^2 (T-\theta)\right]}{\mu_p^2}$$

Since the quantity

$$100\,\frac{m_s X_s (2.84)^2}{\mu_p^2(\Delta m_s - \Delta m_c)} = \text{constant} = K$$

the former reduces to

$$\text{mole percent reduced} = K(\Delta m - \Delta m_c)(T + \theta)$$

where Δm is the apparent mass change, and the subscripts s and c refer to sample and empty container, respectively.

The reaction of sodium metal with Fe_3C, $Fe_{20}C_9$, and $Fe_{2.52}Mn_{0.18}C$ was investigated at elevated temperatures using TMA[193]. It was possible by this technique to follow the disappearance of iron carbide when in contact with the liquid sodium metal, as well as the formation of iron metal or other ferromagnetic species as reaction products.

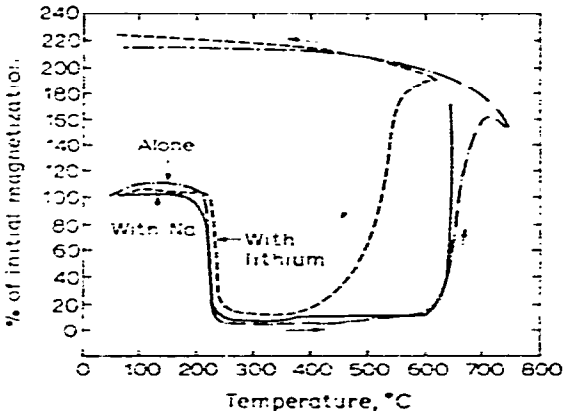

Fig. 5.38. TMA curves of Fe_3C with Na or Li[193].

The TMA curves[193] of Fe_3C with excess sodium or lithium metal are illustrated in Fig. 5.38. Decomposition of Fe_3C alone is rapid above 600 °C while the reaction with sodium metal indicates that no direct reaction such as

$$2Fe_3C + 2Na \rightarrow Na_2C_2 + 6Fe$$

can take place in the temperature range at which the dissociation reaction is important. Both the Curie point and the extent of interaction with the magnetic field at room temperature were found to be unaffected by the heating.

5.10. Photothermal techniques

David[194] described an apparatus in which the photothermal analysis (PTA) and DTA curves of inorganic compounds and organic polymers could be determined. Although the two techniques reinforce each other and provide complementary

information, light emanation from the sample provides information which is generally not present in the DTA curves.

The apparatus used for simultaneous PTA–DTA measurements is shown in Fig. 5.39. The Stone–Premco DTA cell was modified by drilling a 0.275 in. opening in the cell cap to permit sample viewing by the photomultiplier tube. An EMI "end-on" photomultiplier, type 6356S, with a spectral response of 2000–6000 Å, was employed for the measurements. The PTA signal was recorded on one channel of a two-channel potentiometric recorder.

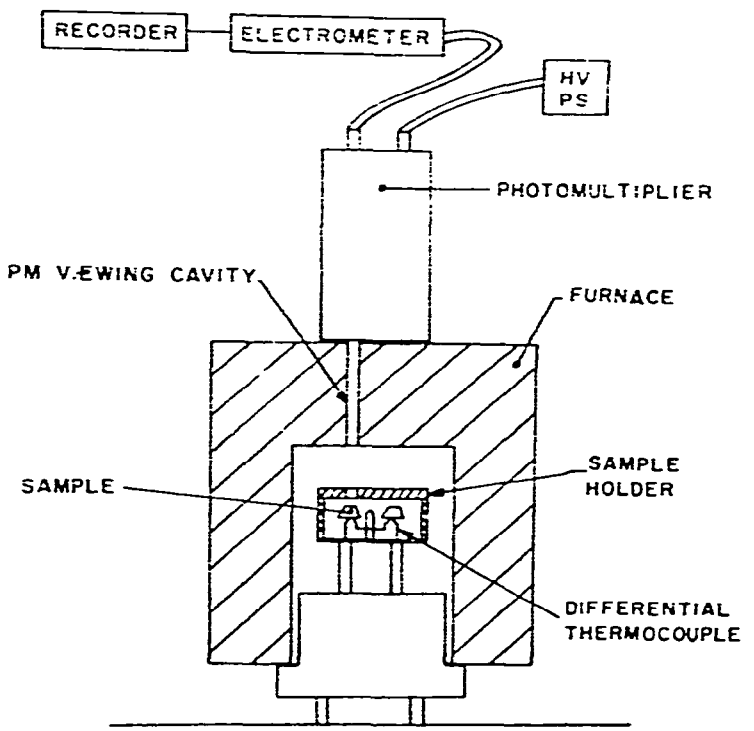

Fig. 5.39. Simultaneous PTA–DTA apparatus used by David[194].

The simultaneous PTA–DTA curves of $CuSO_4 \cdot 5H_2O$ are illustrated in Fig. 5.40. The PTA curve showed a slightly increased response in the 300–400 °C region as compared to the blank run. A small peak was noted in the PTA curve from 225 to 275 °C, which was duplicated in numerous runs of the compounds. The origin of the peak was not given.

A somewhat more sophisticated apparatus for measuring phase transitions of incandescent materials was described by Rupert[195]. In this apparatus, as illustrated in Fig. 5.41, a photomultiplier tube was used to follow the temperature changes of the sample. The phototube responds to the luminosity of the sample, which is proportional to the sample temperature. It is not necessary to know the exact relationship between the output of the phototube and the temperature of the sample because

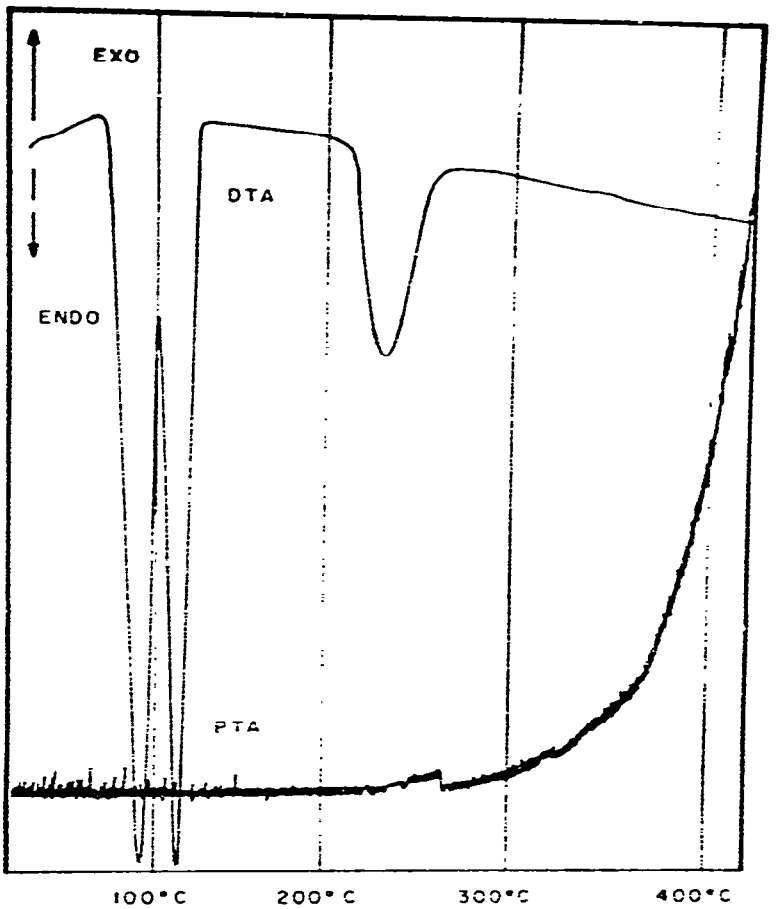

Fig. 5.40. Simultaneous PTA–DTA curves of $CuSO_4 \cdot 5H_2O$; heating rate 10°C/min.

temperature calibration is accomplished by using a calibrated optical pyrometer which receives part of the light from the sample. The sample was contained in a crucible (A) located within the current concentrator (B). The latter receives power from the induction heater (K), whose output is controlled by the induction heater control (J). Light from the sample emerges through a 0.070 in. diameter hole in the top of the crucible, and travels upward through a Pyrex or quartz window into the lower end of the beam splitter. Part of the light is reflected at approximately 90° to the axis of the beam splitter, by the partially aluminized bottom mirror, to the optical pyrometer (D) used to measure the temperature of the sample. The light that passes through the mirror is reflected outward by the top mirror, and is then focused by the 27.5 cm focal length achromatic lens onto a 0.067 in. diameter aperture in front of the photomultiplier tube.

Typical cooling curves studied by this technique include the freezing of a molybdenum carbide–carbon mixture at 2540°C, a cooling curve of the freezing of zirconium carbide–carbon eutectic mixture at 2855°C, and a solid-state transition of uranium dicarbide at 1800°C.

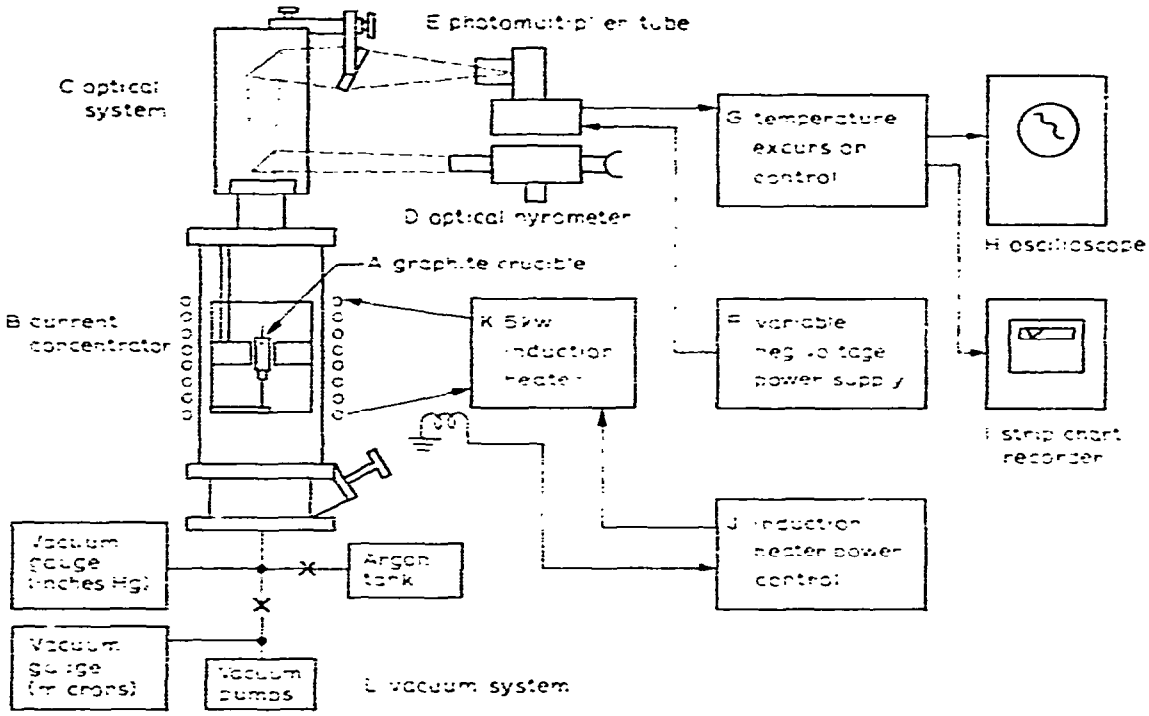

Fig. 5.41. Apparatus used by Rupert[195].

5.11. *Infrared spectroscopy*

Although the KBr disc technique in infrared spectroscopy is well known, few quantitative kinetic studies of solid-state chemical reactions have been reported. Hisatsune and co-workers[196–201] found that many chemical reactions are initiated by heating the discs to elevated temperatures and that the kinetics of these reactions could be conveniently followed by this technique. The discs are placed in an oven for the desired length of time, and the spectrum was recorded after the disc was quenched to room temperature. A typical disc weighing about 0.5 g cooled from about 600°C to room temperature in less than a minute. Discs prepared from potassium salts could be heated in air to about 600°C, but above this temperature appreciable sublimation of the matrix salt occurred. The initial heating usually produced the greatest change in the appearance of the discs. They turned opaque, expanded, and often showed blisters on the surface when gaseous products were formed by the decomposition of the solutes. In some cases, the transparency of the disc could be restored by breaking it into small pieces and repressing. For quantitative work the rim of the expanded disc was sanded off until it fitted the die cavity. Studies reported included the trapping of the BO_2 ion[197], the carbon dioxide anion (CO_2^-) free radical[198], the carbonate anion (CO_3^-) free radical[199], the formate ion from the acetate ion[200], and the decomposition of the perchlorate ion[201].

Wydeven and Leban[202] reported the thermal decomposition kinetics of silver

carbonate using the disc technique. Continuous, in situ quantitative analysis of infrared active reactants and products of the decomposition reactions was made possible by use of a heated cell. The cell was constructed of stainless steel and could be heated to 500 °C with the KRS–F cell windows maintained at room temperature by the flow of cooling water.

A heated cell for infrared spectroscopy was also described by LeRoux and Montano[203] for use up to 200 °C.

A heated programmable cell was used by Tanaka et al.[204] to study the decomposition of a number of cobalt(III) ammine complexes. The disc matrix was either KCl or KBr; at elevated temperatures the discs frequently became opaque to infrared radiation.

5.12. Dynamic reflectance spectroscopy

The total reflected radiation from a mat surface, R_T, consists in general of two components: a regular reflectance component (also called surface or mirror reflection), R, and a diffuse reflection component, R_∞. The former is due to the reflection at the surface of single crystallites while the latter arises from the radiation penetrating into the interior of the solid sample and re-emerging to the surface after being scattered numerous times.

Almost all of the studies in diffuse reflectance spectroscopy have been carried out at ambient temperatures or, in some cases, sub-ambient temperatures. In many cases, a greater amount of information about a chemical system can be attained if the reflectance spectra are obtained at elevated temperatures. Normally, temperatures in the range from 100 to 400 °C have been employed although higher temperatures may also be attained without undue experimental difficulties. Two modes of investigation are used for the high temperature reflectance studies. The first is the measurement of the sample spectra at various fixed or isothermal temperatures: the second is the measurement of the change in reflectance of the sample as a function of the increasing temperature. The first mode is called the static method or *high temperature reflectance spectroscopy*[205] (HTRS); the second is a dynamic method and is called *dynamic reflectance spectroscopy* (DRS)[206]. The DRS curves reveal the temperatures at which sample thermal transitions begin and terminate, and also permit the investigation of only a single thermal transition at a time. It is useful for determining the thermal stability of a substance and also sample structural changes which are a function of temperature. Indeed, this technique shows great promise as a complementary method for other thermal techniques such as TG, DTA, high temperature X-ray diffraction, and so on.

The theory, instrumentation, and applications of HTRS and DRS have been adequately reviewed by Wendlandt[207]. A new controlled atmosphere sample holder has been recently described[208] while Wendlandt and Bradley[209] discussed the simultaneous measurement of DRS with EGD for certain inorganic complexes. Most of the applications of this technique have been in transition metal coordination

chemistry. Compounds that have been investigated include $[Cu(en)(H_2O)]SO_4$[210], $Co(py)_2Cl_2$[210,211], $CuSO_4 \cdot 5H_2O$[210], $CoCl_2 \cdot 6H_2O$[210], and $Ni(py)_4Cl_2$[207]. The thermochromism of the $M_n[HgI_4]$ ($M = Ag^+$, Cu^+, Pb^{2+}, and Hg^{2+}) complexes have also been studied[212].

REFERENCES

1 C. Duval, *Inorganic Thermogravimetric Analysis*, Elsevier, Amsterdam, 1953.
2 C. Duval, *Inorganic Thermogravimetric Analysis*, Second edition, Elsevier, Amsterdam, 1963.
3 W. W. Wendlandt, *Thermal Methods of Analysis*, Interscience–Wiley, New York, 1964.
4 H. C. Anderson, in P. E. Slade and L. T. Jenkins (editors), *Techniques and Methods of Polymer Evaluation*, M. Dekker, New York, 1966.
5 H. Saito, *Thermobalance Analysis*, Gijitsu Shoin, Tokyo, 1962.
6 C. Keattch, *Introduction to Thermogravimetry*, Heyden, London, 1969.
7 F. Paulik and J. Paulik, *Thermoanalysis*, Muszaki Konyvkiado, Budapest, 1963.
8 H. Saito, in R. F. Schwenker and P. D. Garn (editors), *Thermal Analysis*, Vol. 1, Academic Press, New York, 1969, p. 11.
9 W. W. Wendlandt, *Thermal Analysis Instrumentation*, Vol. 2, *Handbook of Commercial Scientific Instruments*, Dekker, New York, in press.
10 S. Gordon and C. Campbell, *Anal. Chem.*, 32 (1960) 271 R.
11 Anonymous, *Sci. Res. (Dacca, Pak.)*, March (1969) 32.
12 A. E. Newkirk, *Anal. Chem.*, 32 (1960) 1558.
13 E. P. Manche and B. Carroll, *Rev. Sci. Instrum.*, 35 (1964) 1486.
14 S. D. Norem, M. J. O'Neill and A. P. Gray, in H. G. McAdie (editor), *Proceedings of the Third Toronto Symposium on Thermal Analysis*, Chemical Institute of Canada, Toronto, 1969, p. 221.
15 S. D. Norem, M. J. O'Neill and A. P. Gray, *Thermochim. Acta*, 1 (1970) 20.
16 A. E. Newkirk, *Thermochim. Acta*, 2 (1971) 1.
17 H. G. Wiedemann, *Chem.-Ing. Tech.*, 11 (1964) 1105.
18 *Mettler Thermal Technique Series*, T 102, 1966.
19 *Mettler Thermal Technique Series*, T 103, 1967.
20 *Mettler Thermal Technique Series*, T 104, 1968.
21 H. G. Wiedemann and A. van Tets, *Naturwissenschaften*, 54 (1967) 442.
22 E. A. Gulbransen, K. F. Andrew and F. A. Brassart, in P. M. Waters (editor), *Vacuum Microbalance Techniques*, Vol. 4, Plenum Press, New York, 1965, p. 127.
23 L. Cahn and N. C. Peterson, *Anal. Chem.*, 39 (1967) 403.
24 L. Cahn and H. Schultz, *Anal. Chem.*, 35 (1963) 1729.
25 H. L. Friedman, *Anal. Chem.*, 37 (1964) 768.
26 J. Šesták, *Talanta*, 13 (1966) 567.
27 J. Šesták, *Silikaty*, 5 (1961) 68.
28 F. Paulik, J. Paulik and L. Erdey, *Talanta*, 13 (1966) 1405.
29 L. Erdey, F. Paulik and J. Paulik, *Mikrochim. Acta*, (1966) 699.
30 J. Paulik, F. Paulik and L. Erdey, *Period. Polytech., Chem. Eng.*, 12 (1968) 105.
31 H. G. Wiedemann, *Chem. Ing. Tech.*, 36 (1964) 1105.
32 H. G. Wiedemann, A. van Tets and H. P. Vaughan, *Pittsburgh Conference on Analytical Chemistry*, Pittsburgh, Pa., February 21, 1966.
33 H. G. Wiedemann, in R. F. Schwenker and P. D. Garn (editors), *Thermal Analysis*, Vol. 1, Academic Press, New York, 1969, p. 229.
34 H. G. McAdie, *Anal. Chem.*, 35 (1963) 1840.
35 J. W. Smith and D. R. Johnson, in R. F. Schwenker and P. D. Garn (editors), *Thermal Analysis*, Vol. 2, Academic Press, New York, 1969, p. 1251.
36 M. Ramakrishna Udupa and S. Aravamundan, *Current Sci.*, 39 (1970) 206.
37 W. W. Wendlandt, in H. G. McAdie (editor), *Proceedings of the First Tororto Symposium on Thermal Analysis*, Chemical Institute of Canada, Toronto, 1965, p. 101.
38 R. Maurer and H. G. Wiedemann, in R. F. Schwenker and P. D. Garn (editors), *Thermal Analysis*, Vol. 1, Academic Press, New York, 1969, p. 177.

39 J. Chiu, *Thermochim. Acta*, 1 (1970) 231.
40 J. Chiu, *Anal. Chem.*, 40 (1968) 1516.
41 H. Saito, R. Otsuka, S. Iwata and K. Tsuchimoto, *Waseda Univ. Bull. Sci., Eng. Lab.*, 27 (1964) 26.
42 T. L. Chang and T. E. Mead, *Anal. Chem.*, 43 (1971) 534.
43 E. K. Gibson and S. M. Johnson, *Thermochim. Acta*, 4 (1973) 49.
44 E. K. Gibson, *Thermochim. Acta*, 7 (1973) 243.
45 F. Zitomer, *Anal. Chem.*, 40 (1968) 1091.
46 D. E. Wilson and F. M. Hamaker, in R. F. Schwenker and P. D. Garn (editors), *Thermal Analysis*, Vol. 2, Academic Press, New York, 1969, p. 1251.
47 J. Paulik and F. Paulik, *Thermochim. Acta*, 3 (1971) 13.
48 J. Paulik and F. Paulik, *Thermochim. Acta*, 3 (1971) 17.
49 J. Paulik and F. Paulik, *Proceedings of the Third Anal. Chemical Conference*, Vol. 2, Academai Kaido, Budapest, August 24–29, 1970, p. 225.
50 R. Franck and M. Harmelin, *ibid.*, p. 219.
51 G. A. Kleineberg and D. L. Geiger, in H. G. Wiedemann (editor), *Thermal Analysis (Proc. ICTA III)*, Vol. 1, Birkhäuser Verlag, Basel, 1972, p. 325.
52 H. G. Wiedemann, in H. G. Wiedemann (editor), *Thermal Analysis, (Proc. ICTA III)*, Vol. 1, Birkhäuser Verlag, Basel, 1972, p. 171.
53 H. G. Wiedemann, *Thermochim. Acta*, 3 (1972) 355.
54 M. R. Lorenz and G. J. Janz, *J. Chem. Educ.*, 40 (1963) 611.
55 N. J. Olson, in R. F. Schwenker and P. D. Garn (editors), *Thermal Analysis*, Vol. 1, Academic Press, New York, 1969, p. 325.
56 E. Steinheil, in H. G. Wiedemann (editor), *Thermal Analysis*, Vol. 1, Birkhäuser Verlag, Basel, 1972, p. 187.
57 H. A. Brown, E. C. Penski and J. J. Callahan, *Thermochim. Acta*, 3 (1972) 271.
58 R. W. Harrison and E. J. Delgrasso, *J. Sci. Instrum.*, 41 (1964) 222.
59 E. Peuersen, *J. Sci. Instrum.*, 1 (1968) 1013.
60 W. S. Bradley and W. W. Wendlandt, *Anal. Chem.*, 43 (1971) 223.
61 W. W. Wendlandt, *Chimia*, 26 (1972) 2.
62 W. J. Smothers and Y. Chiang, *Differential Thermal Analysis: Theory and Pratice*, Chemical Publ. Co., New York, 1958.
63 W. J. Smothers and Y. Chiang, *ibid.*, Second edition, 1966.
64 P. D. Garn, *Thermoanalytical Methods of Investigation*, Academic Press, New York, 1965.
65 D. Schultze, *Differentialthermoanalyse*, Deutscher Verlag der Wissenschaften, Berlin, 1969.
66 R. C. Mackenzie (editor), *Differential Thermal Analysis*, Vol. 1, Academic Press, New York, 1970.
67 C. B. Murphy, *Anal. Chem.*, 44 (1972), 513R.
68 S. Gordon, *J. Chem. Educ.*, 40 (1963) A87.
69 W. W. Wendlandt, *Lab. Manag.*, October (1965) 26.
70 H. G. Wiedemann and A. van Tets, *Z. Anal. Chem.*, 233 (1968) 161.
71 H. G. Wiedemann, *Mettler Thermal Technique Series*, Bulletin T 106.
72 H. G. Wiedemann, *Z. Anal. Chem.*, 220 (1966) 1.
73 T. Ozawa, *Bull. Chem. Soc. Jap.*, 39 (1966) 2071.
74 T. Ozawa, M. Momota, and H. Isozaki, *Bull. Chem. Soc. Jap.*, 40 (1967) 1583.
75 T. Ozawa, H. Isozaki and A. Negishi, *Thermochim. Acta*, 1 (1970) 545.
76 E. J. Barrett, H. W. Hoyer and A. V. Santoro, *Mikrochim. Acta*, (1970) 1121.
77 A. V. Santoro, E. J. Barrett and H. W. Hoyer, *J. Thermal Anal.*, 2 (1970) 461.
78 W. W. Wendlandt, *Thermochim. Acta*, 1 (1970) 419.
79 M. D. Karkhanavala, V. V. Deshpande and A. B. Phadnis, *J. Thermal Anal.*, 2 (1970) 259.
80 F. W. Wilburn, J. R. Hesford and J. R. Flower, *Anal. Chem.*, 40 (1968) 777.
81 R. Melling, F. W. Wilburn and R. M. McIntosh, *Anal. Chem.*, 41 (1969) 1275.
82 L. G. Berg and V. P. Egunov, *J. Thermal Anal.*, 1 (1969) 441.
83 E. L. Dosch, *Thermochim. Acta*, 1 (1970) 367.
84 W. H. King, A. F. Findeis and C. T. Camilli, in R. J. Porter and J. F. Johnson (editors), *Analytical Colorimetry*, Plenum Press, New York, Vol. 1, 1968, p. 261.
85 W. H. King, C. T. Camilli and A. F. Findeis, *Anal. Chem.*, 40 (1968) 1330.

86 E. M. Bollin and A. J. Bauman, in R. J. Porter and J. F. Johnson (editors), *Analytical Colorimetry*, Vol. 2, Plenum Press, New York, 1970, p. 339.
87 D. J. David, D. A. Ninke and B. Duncan, *Amer. Lab.*, January (1971) 31.
88 L. G. Berg and V. P. Eganov, *J. Thermal Anal.*, 2 (1970) 53.
89 R. J. Harker, *Amer. Mineral.*, 49 (1964) 1741.
90 L. H. Cohen, W. Klement and G. C. Kennedy, *J. Phys. Chem. Solids*, 27 (1966) 179.
91 M. Kubalia and G. M. Schneider, *Ber. Bunsenges. Phys. Chem.*, 75 (1971) 513.
92 S. Ueda, S. Yokoyama, T. Ishii and G. Takeya, *Kogyo Kogaku Zasshi*, 74 (1971) 1377.
93 G. Takeya, T. Ishii, K. Makino and S. Ueda, *Kogyo Kogaku Zasshi*, 69 (1966) 1654.
94 D. J. David, *Anal. Chem.*, 37 (1965) 82.
95 P. D. Garn, *Anal. Chem* 37 (1965) 77.
96 C. E. Locke, in H. G. McAdie (editor), *Proceedings of Third Toronto Symposium on Thermal Analysis*, Chemical Institute of Canada, Toronto, Feb. 25–26, 1969, p. 251.
97 H. R. Kemme and S. I. Kreps, *Anal. Chem.*, 41 (1969) 1869.
98 G. P. Morie, T. A. Powers and C. A. Glover, *Thermochim. Acta*, 3 (1972) 259.
99 R. L. Bohon, in H. G. McAdie (editor), *Proceedings of Third Toronto Symposium on Thermal Analysis*, Chemical Institute of Canada, Toronto, Feb. 25–26, 1969, p. 33.
100 J. P. Redfern and B. L. Treherne, in H. G. Wiedemann (editor), *Thermal Analysis*, Vol. I, Birkhäuser Verlag, Basel, 1972, p. 55.
101 S. A. Wald and C. C. Winding, *Anal. Chem.*, 37 (1965) 1622.
102 T. Fujino, T. Kurosawa, Y. Miyata and K. Naito, *J. Phys. E*, 4 (1971) 51.
103 T. Ozawa, *Nippon Kagaku Zasshi*, 88 (1967) 532.
104 R. Dimitrov, *Dokl. Bulg. Akad. Nauk*, 23 (1970) 1215.
105 J. Šesták, E. Burda, P. Holba and A. Bergstein, *Chem. Listy*, 63 (1969) 785.
106 G. N. Rupert, *Rev. Sci. Instrum.*, 36 (1965) 1629.
107 L. O. Gilpatrick, S. Cantor and C. J. Barton, in R. F. Schwenker and P. D. Garn (editors), *Thermal Analysis*, Academic Press, New York, 1969, p. 85.
108 A. Yamamoto, K. Yamada, M. Maruta and J. Akiyama, in R. F. Schwenker and P. D. Garn (editors), *Thermal Analysis*, Academic Press, New York, 1969, p. 105.
109 E. M. Bollin, in R. F. Schwenker and P. D. Garn (editors), *Thermal Analysis*, Academic Press, New York, 1969, p. 255.
110 J. T. Burr, in R. F. Schwenker and P. D. Garn (editors), *Thermal Analysis*, Academic Press, New York, 1969, p. 301.
111 W. W. Wendlandt and W. S. Bradley, *Anal. Chim. Acta*, 52 (1970) 397.
112 M. J. O'Neill, *Anal. Chem.*, 36 (1964) 1238.
113 E. S. Watson, M. J. O'Neill, J. Justin and N. Brenner, *Anal. Chem.*, 36 (1964) 1233.
114 *Perkin–Elmer Thermal Analysis Newsletter*, No. 10, Feb. 1972.
115 M. J. O'Neill and R. L. Fyans, *Eastern Analytical Symposium*, New York, Nov. 1971.
116 M. J. O'Neill and A. P. Gray, in H. G. Wiedemann (editor), *Thermal Analysis*, Vol. I, Birkhäuser Verlag, Basel, 1972, p. 279.
117 F. E. Freeberg and T. G. Alleman, *Anal. Chem.*, 38 (1966) 1806.
118 W. W. Wendlandt, *Anal. Chim. Acta*, 49 (1970) 187.
119 R. E. Farritor and L. C. Tao, *Thermochim. Acta*, 1 (1970) 297.
120 I. Mita, I. Imai and H. Kambe, *Thermochim. Acta*, 2 (1971) 337.
121 G. P. Morie, T. A. Powers and C. A. Glover, *Thermochim. Acta*, 3 (1972) 259.
122 R. A. Baxter, in R. F. Schwenker and P. D. Garn (editors), *Thermal Analysis*, Vol. 1, Academic Press, New York, 1969, p. 65.
123 P. F. Levy, G. Nieuweboer and L. C. Semanski, *Thermochim. Acta*, 1 (1970) 429.
124 D. J. David, *J. Thermal Anal.*, 3 (1971) 247.
125 R. C. Wilhoit, *J. Chem. Educ.*, 44 (1967) 571.
126 E. L. Dosch and W. W. Wendlandt, *Thermochim. Acta*, 1 (1970) 181.
127 W. J. Evans, E. J. McCourtney and W. B. Carney, *Anal. Chem.*, 40 (1968) 262.
128 E. Calvet, *C.R. Acad. Sci.*, 226 (1948) 1702.
129 F. R. Sale, *J. Phys. E*, 3 (1970) 646.
130 C. N. Thomasson and D. A. Cunningham, *J. Sci. Instrum.*, 41 (1964) 308.
131 C. Berger, M. Richard and L. Eyraud, *Bull. Soc. Chim. Fr.*, (1965) 1491.
132 A. Roux, M. Reebaid, L. Eyraud and J. Elston, *J. Phys. Phys. Appl.*, 25 (1964) 51A.

133 P. S. Nicholson, *E.O. Lawrence Radiation Lab. Report*, UCRL–17820, Sept. 1967.
134 D. M. Speros and R. L. Woodhouse, *J. Phys. Chem.*, 67 (1963) 2164.
135 D. M. Speros and R. L. Woodhouse, *J. Phys. Chem.*, 72 (1968) 2846.
136 H. Garski, *Z. Angew. Chemie*, 24 (1968) 206.
137 W. Muller and D. Schuller, *Ber. Bunsenges. Phys. Chem.*, 75 (1971) 79.
138 W. Lodding (editor), *Gas Effluent Analysis*, M. Dekker, New York, 1967.
139 A. S. Kenyon, in P. E. Slade and L. T. Jenkins (editors). *Techniques and Methods of Polymer Evaluation*, M. Dekker, New York, 1966, Chapt. 5.
140 J. Paulik, F. Paulik and L. Erdey, *Mikrochim. Acta*, (1966) 887.
141 J. Paulik and F. Paulik, *Talanta*, 17 (1970) 1224.
142 F. Paulik and J. Paulik, in *Proceedings of the Third Analytical Chemical Conference*, Budapest, Hungary, 1970, p. 225.
143 J. Paulik and F. Paulik, in *Proceedings of the Third Analytical Chemical Conference*, Budapest, Hungary, 1970, p. 231.
144 P. Marik, E. Buzagh, J. Inczeoy, J. Paulik and L. Erdey, in *Proceedings of the Third Analytical Chemical Conference*, Budapest, Hungary, 1970, p. 233.
145 A. B. Kiss, *Acta Chim. (Budapest)*, 61 (1969) 207.
146 A. B. Kiss, *Acta Chim. (Budapest)*, 63 (1970) 243.
147 G. M. Bancroft and H. D. Gesser, *J. Inorg. Nucl. Chem.*, 27 (1965) 1537.
148 J. N. Maycock and V. R. Pai Verneker, *Anal. Chem.*, 40 (1968) 1935.
149 R. P. Turcotte, T. D. Chikalla and L. Eyring, *Anal. Chem.*, 43 (1971) 958.
150 J. Guenot, J. L. Valicon and G. Pannetier, *Bull. Soc. Chim. Fr.*, (1967) 3068.
151 J. Thomas, G. M. Hieftje and D. E. Orlopp, *Anal. Chem.*, 37 (1965) 762.
152 P. D. Garn, *Talanta*, 11 (1964) 1417.
153 J. Franc and J. Pour, *Anal. Chim. Acta*, 43 (1969) 129.
154 H. Juntgen and K. H. van Heek, *Fuel*, 47 (1968) 103.
155 F. E. Austin, J. Dollimore and B. H. Harrison, in R. F. Schwenker and P. D. Garn (editors), *Thermal Analysis*, Vol. 1, Academic Press, New York, 1969, p. 311.
156 F. Chantret, *Bull. Soc. Fr. Mineral. Cristallogr.*, 92 (1969) 462.
157 G. K. Skala, *Anal. Chem.*, 35 (1963) 702.
158 C. B. Murphy, F. W. Van Luik and A. C. Pitsas, *Plast. Des. Process.*, July (1964) 16.
159 C. B. Murphy, *J. Sci. Instrum.*, 41 (1964), p. 195.
160 F. T. Eggertsen, E. E. Seibert and F. H. Stross, *Anal. Chem.*, 41 (1969) 1175.
161 F. T. Eggertsen, H. M. Jaki and F. H. Stross, in R. F. Schwenker and P. D. Garn (editors), *Thermal Analysis*, Vol. 1, Academic Press, New York, 1969, p. 341.
162 F. T. Eggertsen and F. H. Stross, *Thermochim. Acta*, 1 (1970) 451.
163 J. Chiu, *Anal. Chem.*, 39 (1967) 861.
164 D. J. David, *Thermochim. Acta*, 1 (1970) 277.
165 W. W. Wendlandt, *Thermochim. Acta*, 1 (1970) 11.
166 H. J. Borchardt and F. Daniels, *J. Phys. Chem.*, 61 (1957) 917.
167 J. Chiu, *J. Polym. Sci.*, C5 (1965) 27.
168 W. K. Rudloff and E. S. Freeman, *J. Phys. Chem.*, 74 (1970) 3317.
169 M. D. Judd and M. I. Pope, *J. Appl. Chem.*, 20 (1970) 280.
170 R. W. Carroll and R. V. Mangravite, in R. F. Schwenker and P. D. Garn (editors), *Thermal Analysis*, Vol. 1, Academic Press, New York, 1969, p. 189.
171 W. C. McCrone, *Application of Thermal Microscopy*, Tech. Bulletin No. 3003, Mettler Instr. Corp., 1968.
172 W. C. McCrone, *Fusion Methods in Chemical Microscopy*, Interscience, New York, 1957.
173 L. Kofler and A. Kofler, *Thermo-Mikro-Methoden*, Wagner, Innsbruck, 1957.
174 H. A. Vaughan, *Thermochim. Acta*, 1 (1970) 111.
175 A. van Tets and H. G. Wiedemann, in R. F. Schwenker and P. D. Garn (editors), *Thermal Analysis*, Vol. 1, Academic Press, New York, 1969, p. 121.
176 L. Verbit and T. R. Halbert, *J. Chem. Educ.*, 48 (1971) 773.
177 J. A. Robertson, unpublished report, 1970.
178 H. P. Bruckner and K. Heide, *Z. Chem.*, 10 (1970) 125.
179 B. D. Faubion, *Anal. Chem.*, 43 (1971) 241.
180 A. K. Kolb, C. L. Lee and R. M. Trail, *Anal. Chem.*, 39 (1967) 1206.

181 G. W. Miller, *Thermochim. Acta*, 3 (1972) 467.
182 R. P. Miller and G. Sommer, *J. Sci. Instrum.*, 43 (1966) 293.
183 G. Sommer, *Instrum. Tech. in Southern Africa*, 2 (1965) 10.
184 G. Sommer, P. R. Jochens and D. D. Howat, *J. Phys. E*, 1 (1968) 1116.
185 G. Sommer and P. R. Jochens, *Miner. Sci. Eng.*, 3 (1971) 3.
186 V. Balek, *J. Mater. Sci.*, 4 (1969) 919.
187 V. Balek, *Anal. Chem.*, 42 (1970) 16A.
188 V. Balek, *Glas. Hem. Drus.*, Beograd, 34 (1969) 345.
189 V. Balek and K. B. Zaborenko, *Radiokhimiia*, 10 (1968) 450.
190 K. E. Hyde, *J. Chem. Educ.*, 49 (1972) 69.
191 L. N. Mulay and L. K. Keys, *Anal. Chem.*, 36 (1964) 2383.
192 E. L. Simmons and W. W. Wendlandt, *Anal. Chim. Acta*, 35 (1966) 461.
193 R. G. Charles, L. N. Yannopoulas and P. G. Haverlack, *J. Inorg. Nucl. Chem.*, 32 (1970) 447.
194 D. J. David, *Thermochim. Acta*, 3 (1972) 277.
195 G. N. Rupert, *Rev. Sci. Instrum.*, 34 (1963) 1183.
196 I. C. Hisatsune, *Perkin–Elmer Instrument News*, 16 (1965) No. 2, p. 2.
197 I. C. Hisatsune and N. Haddock Suarez, *Inorg. Chem.*, 3 (1964) 168.
198 K. O. Hartman and I. C. Hisatsune, *J. Chem. Phys.*, 44 (1966) 1913.
199 I. C. Hisatsune, T. Adl, E. C. Beahm and R. J. Kempf, *J. Phys. Chem.*, 74 (1970) 3225.
200 I. C. Hisatsune, E. C. Beahm and R. J. Kempf, *J. Phys. Chem.*, 74 (1970) 3444.
201 I. C. Hisatsune and D. G. Linnnehan, *J. Phys. Chem.*, 74 (1970) 4091.
202 T. Wydeven and M. Leban, *Anal. Chem.*, 40 (1968) 363.
203 J. H. LeRoux and J. J. Montano, *Anal. Chem.*, 38 (1966) 1807.
204 N. Tanaka, M. Sato and M. Nanjo, *Sci. Reports Tohoku Univ.*, 48 (1964) 1.
205 W. W. Wendlandt, P. H. Franke and J. P. Smith, *Anal. Chem.*, 35 (1963) 105.
206 W. W. Wendlandt, *Science*, 140 (1963) 1085.
207 W. W. Wendlandt, *Pure Appl. Chem.*, 25 (1971) 825.
208 W. W. Wendlandt and E. L. Dosch, *Thermochim. Acta*, 1 (1970) 103.
209 W. W. Wendlandt and W. S. Bradley, *Thermochim. Acta*, 1 (1970) 143.
210 W. W. Wendlandt, in W. W. Wendlandt (editor), *Modern Aspects of Reflectance Spectroscopy*, Plenum, New York, 1968.
211 W. W. Wendlandt, *J. Thermal Anal.*, 2 (1970) 469.
212 W. W. Wendlandt and W. S. Bradley, *Thermochim. Acta*, 1 (1970) 529.